



TALLINN UNIVERSITY OF TECHNOLOGY  
SCHOOL OF ENGINEERING  
DEPARTMENT OF MATERIALS AND ENVIRONMENTAL TECHNOLOGY

**APPLICATION OF FERROCENE AEROGEL AND  
IRON-DOPED ORGANIC AEROGEL IN FENTON-  
LIKE AND PHOTOLYTIC PROCESSES FOR  
OXIDATION OF N-NITROSODIETHYLAMINE AND  
TRIMETHOPRIM IN WATER - A COMPARATIVE  
STUDY**

**FERROTSEENAEROGEEELI JA RAUAGA LEGEERITUD  
ORGAANILISE AEROGEEELI RAKENDAMINE FENTON-  
TÜÜPI JA FOTOLÜÜTILISTES PROTSESSIDES N-  
NITROSODIETÜÜLAMIINI JA TRIMETOPRIMI  
LAGUNDAMISEKS VEES - VÕRDLEV UURING**

MASTER THESIS

Student: Sofia Pereskoka

Student code: 192274KAKM

Supervisor: Maarja Kask, junior researcher

Co-supervisor: Juri Bolobajev, researcher

Tallinn 2021

## **AUTHOR'S DECLARATION**

Hereby I declare, that I have written this thesis independently.

No academic degree has been applied for based on this material. All works, major viewpoints and data of the other authors used in this thesis have been referenced.

"26" May 2021

Author: Sofia Pereskoka

*/ signature/*

Thesis is in accordance with terms and requirements

"26" May 2021

Supervisor: Maarja Kask

*/signature/*

Co-supervisor: Juri Bolobajev

*/signature/*

Accepted for defence

".....".....20... .

Chairman of theses defence commission: Marina Trapido

*/name and signature/*

**Non-exclusive Licence for Publication and Reproduction of  
Graduation Thesis<sup>1</sup>**

I, Sofia Pereskoka (date of birth: 3.10.1996 )

hereby

1. grant Tallinn University of Technology (TalTech) a non-exclusive license for my thesis

Application of ferrocene aerogel and iron-doped organic aerogel in Fenton-like and photolytic processes for oxidation of N-nitrosodiethylamine and trimethoprim in water - a comparative study,

supervised by

Maarja Kask and Juri Bolobajev,

1.1 reproduced for the purposes of preservation and electronic publication, incl. to be entered in the digital collection of TalTech library until expiry of the term of copyright;

1.2 published via the web of TalTech, incl. to be entered in the digital collection of TalTech library until expiry of the term of copyright.

1.3 I am aware that the author also retains the rights specified in clause 1 of this license.

2. I confirm that granting the non-exclusive license does not infringe third persons' intellectual property rights, the rights arising from the Personal Data Protection Act or rights arising from other legislation.

<sup>1</sup> Non-exclusive Licence for Publication and Reproduction of Graduation Thesis is not valid during the validity period of restriction on access, except the university`s right to reproduce the thesis only for preservation purposes.

/signature/

26.05.2021

**DEPARTMENT OF MATERIALS AND ENVIRONMENTAL TECHNOLOGY**

**THESIS TASK**

**Student:** Sofia Pereskoka, 192274KAKM

Study programme, main speciality: KAKM02/18 - Keemia- ja keskkonnakaitse tehnoloogia

Supervisor: junior researcher, Maarja Kask, 620 2824

Co-supervisor: researcher, Juri Bolobajev, 620 2851

**Thesis topic:**

Application of ferrocene aerogel and iron-doped organic aerogel in Fenton-like and photolytic processes for oxidation of N-nitrosodiethylamine and trimethoprim in water - a comparative study

Ferrotseenaerogeeli ja rauaga legeritud orgaanilise aerogeeli rakendamine Fenton-tüüpi ja fotolüütilistes protsessides N-nitrosodietüülamiini ja trimetoprimi lagundamiseks vees - võrdlev uuring

**Thesis main objectives:**

1. Conduction of experiments with trimethoprim and N-nitrosodiethylamine
2. Conduction of aerogel synthesis
3. Compilation of master thesis

**Thesis tasks and time schedule:**

No	Task description	Deadline
1.	Compilation of literature review	31.03.2021
2.	Compilation of materials and methods	15.04.2021
3.	Compilation of results and discussion	30.04.2021
4.	Compilation of introduction and summary	20.05.2021

**Language:** English **Deadline for submission of thesis:** "26" May 2021

**Student:** Sofia Pereskoka "26" May 2021

*/signature/*

**Supervisor:** Maarja Kask ..... "26" May 2021

*/signature/*

**Co-supervisor:** Juri Bolobajev ..... "26" May 2021

*/signature/*

**Head of study programme:** Marina Trapido ..... " " ..... 2021

*/signature/*

## CONTENTS

PREFACE .....	6
List of abbreviations and symbols .....	7
List of figures .....	9
List of tables .....	10
INTRODUCTION.....	11
1 LITERATURE REVIEW .....	12
1.1 Micropollutants – an invisible threat .....	12
1.2 NDEA and TMP as study objects.....	15
1.3 Advanced oxidation processes in wastewater treatment.....	17
1.3.1 Photolytic processes.....	18
1.3.2 Chemical processes.....	19
1.3.3 Photochemical processes .....	21
1.3.4 Physical processes .....	21
1.3.5 Photocatalytic processes.....	22
1.4 Aerogels .....	25
1.5 Metal aerogels.....	29
2 MATERIALS AND METHODS.....	34
2.1 Reagents and chemicals .....	34
2.2 Experimental setup of photo-induced degradation of pollutants .....	34
2.3 Fenton reaction experiments .....	35
2.4 Determination of a quantum yield .....	36
2.5 Analysis equipment and methods.....	37
2.6 Ferrocene aerogel synthesis .....	37
3 RESULTS AND DISCUSSION .....	40
3.1 Photo-induced degradation of NDEA.....	40
3.2 Photo-induced degradation of TMP .....	42
3.3 Actinometry and quantum yield .....	45
3.4 Fenton experiments .....	47
3.4.1 Experiments with NDEA.....	47
3.4.2 Experiments with TMP .....	49
SUMMARY.....	52
KOKKUVÖTE .....	54
LIST OF REFERENCES .....	55

## **PREFACE**

The thesis topic was initiated by Maarja Kask (junior researcher) and Juri Bolobajev (researcher), the practical work was done at the Laboratory of Environmental Technology of the Department of Materials and Environmental Technology of Taltech. Supervisors M. Kask and J. Bolobajev assisted me in data collecting, consulted and encouraged.

I would like to gratitude my supervisors for assistance, support and inspiration, I am excited to work with wonderful people as them. Also, I gratitude professors of TalTech for interesting courses that gave me knowledge about environmental technology and passion to this field of study. I would like to mention my classmates, who made studying joyful, I am grateful to meet all these people in my life. I would like to thank my family, friends and my beloved man Alexander Vihviläinen for supporting me during this tough but interesting way to graduation.

Tallinn, May 2021

Thesis is about aerogels application in advanced oxidation processes for degradation of trimethoprim and N-nitrosodiethylamine.

Key words: ferrocene aerogel, trimethoprim, N-nitrosodiethylamine, master thesis

## List of abbreviations and symbols

$1-10^{\epsilon[A]}$	the light absorbed by the actinometric solution
5MR	5-methylresorcynol
A	electron acceptor
$A^-$	reduced product
AOPs	advanced oxidation processes
APD	ambient pressure drying
atm	standard atmosphere
C	obtained concentration
$C_0$	initial concentration
CA	cellulose acetate
CB	conductance band
CO <sub>2</sub> -RR	CO <sub>2</sub> reduction reaction
CPD	critical point drying
D	electron donor
$D^+$	oxidised product
DBPs	disinfection by-products
DNA	deoxyribonucleic acid
$e^-$	electron
E <sub>bg</sub>	band gap energy
FD	freeze drying
FeA	ferrocene aerogel
FeOA	iron-doped organic aerogel
Ferrc	ferrocenylmethanol
$h^+$	hole in the valence band
HCHO	formaldehyde
HO•	hydroxyl radical
HO <sub>2</sub> •	hydroperoxyl radical
HPLC	high performance liquid chromatography
h $\nu$	photons
I	radiation intensity in reactor
IUPAC	International Union of Pure and Applied Chemistry
K	kelvin
k	the reaction rate constant
MPs	micropollutants
N	number of moles
$N_A$	Avogadro constant
NDBA	N-nitrosodibutylamine

NDEA	N-nitrosodiethylamine
NDMA	N-nitrosodimethylamine
NDPA	N-nitrosodipropylamine
NDPhA	N-nitrosodiphenylamine
NMEA	N-nitrosomethylethylamine
NMOR	N-nitrosomorpholine
NPip	N-nitrosopiperidine
NPYR	N-nitrosopyrrolidine
pH	potential of hydrogen
pKa	acid dissociation constant
PTFE	polytetrafluoroethylene
SC	semiconductor
SMX	sulfamethoxazole
SPME	solid phase microextraction
t	temperature; time
TMP	trimethoprim
UIO-66	metal organic framework made of $Zr_6O_4(OH)_4$ and 1,4-benzodicarboxylic acid
UV	ultraviolet
UV/Vis	ultraviolet/visible light
UV-A/FeOA	photo-induced degradation with iron-doped organic aerogel
UV-A/FerrA	photo-induced degradation with ferrocene aerogel
UV-C/FerrA	photo-induced degradation with ferrocene aerogel
V	volume; volt
VB	valence band
VUV	vacuum ultraviolet
WHO	World Health Organization
wt%	percentage by weight
w/w	weight by weight
$\Delta N_t$	concentration decrease caused by photolysis per unit of time
$\Delta$	difference
$\Lambda$	wavelength
$\Phi$	quantum yield
$\Phi_{Fe}$	the quantum yield of ferrioxalate

## List of figures

Figure 1. Sources and fates of micropollutants in aquatic environments (Wilkinson et al., 2017) .....	12
Figure 2. Molecular structure of NDEA (National Center for Biotechnology Information, 2021a) .....	15
Figure 3. Formation mechanism of NDMA and NDEA as a result of chloramination (Kodamatani et al., 2021) .....	16
Figure 4. Molecular structure of TMP (National Center for Biotechnology Information, 2021b) .....	17
Figure 5. Classification of advanced oxidation processes (Chirwa & Bamuzza-Pemu, 2010).....	18
Figure 6. Electron-hole pair formation over a semiconductor particle (Chirwa & Bamuzza-Pemu, 2010) .....	23
Figure 7. Energetics of semiconductor photocatalysis, where CB - conductance band, VB - valence band, SC - semiconductor (Chirwa & Bamuzza-Pemu, 2010).....	24
Figure 8. 3D structure of gold aerogels (Burpo et al., 2017).....	25
Figure 9. Silica aerogel protects flower from heat of Bunsen burner (Condliffe, 2014).....	28
Figure 10. 3D model of the batch photo-reactor. 1 - UV lamp; 2 - external cooling jacket; 3-thermometer; 4 - quartz tube; 5 - sampling port (Kask, 2017).....	35
Figure 11. a) Sol-gel process in thermostat; b) resultant ferrocene-gels immersed in acetone .....	39
Figure 12. Comparison of photolytic and photo-induced degradation of N-nitrosodiethylamine FeOA stands for iron-doped organic aerogel, FeA for ferrocene aerogel.....	40
Figure 13. Photoinduced degradation of trimethoprim FeOA stands for iron-doped organic aerogel, FeA for ferrocene aerogel .....	43
Figure 14. Light absorption spectrum of trimethoprim at neutral pH (Kask, 2017).....	44
Figure 15. Fe(II) moles formed from ferrioxalate under the irradiation with UV-A and UV-C light.....	45
Figure 16. Results of Fenton and Fenton-like reactions experiments with NDEA FeOA stands for iron-doped organic aerogel, FerrA for ferrocene aerogel .....	48
Figure 17. Results of Fenton and Fenton-like degradation of TMP FerrA/H <sub>2</sub> O <sub>2</sub> stands for Fenton-like degradation with ferrocene aerogel FeOA/H <sub>2</sub> O <sub>2</sub> stands for Fenton-like degradation with iron-doped organic aerogel.....	49

## List of tables

Table 1. Properties of NDEA (National Center for Biotechnology Information, 2021a)	15
Table 2. Properties of TMP (National Center for Biotechnology Information, 2021b)	..17
Table 3. Data for ferrocene aerogels synthesis .....	38
Table 4. Reaction rate constants for applied photo-induced degradation methods of N-nitrosodiethylamine UV-A/FerrA stands for photo-induced degradation with ferrocene aerogel UV-A/FeOA stands for photo-induced degradation with iron-doped organic aerogel R is the correlation coefficient for linear regression .....	41
Table 5. Reaction rate constants for applied photo-induced degradation methods of trimethoprim UV-C/FerrA stands for photo-induced degradation with ferrocene aerogel R is the correlation coefficient for linear regression .....	43
Table 6. Results of actinometry for UV-A and UV-C lamps.....	46
Table 7. Quantum yields of NDEA under UV-A irradiation and TMP under UV-C irradiation.....	46

## **INTRODUCTION**

Over the last century, the rapid development of industry has led to increasing challenges related to environmental protection. Among them is the contamination of water bodies with micropollutants. Micropollutants are organic or inorganic substances, the presence of which can affect the environment in a negative way even at extremely low concentrations, e.g. in the range of micro, nano, and pico-grams. Given research has been focused on two micropollutants from different classes: antibiotic trimethoprim (TMP) and nitrosoamine N-nitrosodiethylamine (NDEA). It is known that contamination of water bodies with antibiotics leads to antibiotic resistance of microorganisms, which is a subject of growing concern nowadays. Nitrosoamines are carcinogenic and treating health of the human population. Advanced oxidation processes could serve as a promising solution in order to deal with this serious issue.

With respect to aerogels, these materials are unique and relatively new substances with less than 100 years history. Aerogels have found an application in different fields of science and engineering including environmental technology. In the present study, two types of aerogels were explored, i.e. ferrocene aerogel and iron-doped organic aerogel. Recently, metal-doped organic aerogels were implemented in the study of Bolobajev, Kask & Koel (2019), where aerogels showed ability to induce the photo-degradation of antibiotic trimethoprim. Ferrocene aerogel is a new substance, which application in environmental technology has not been studied yet. Therefore, the present master thesis comprises a study on the photo-induced degradation of NDEA and TMP in the presence of aerogels.

For degradation of studied substances photolysis, photo-induced process with aerogels as catalysts, classical Fenton and Fenton-like process with aerogels were studied. The aim of this study is to explore application of aerogels in environmental technology.

According to that, the following hypotheses have been set:

H1: Studied aerogels are able to induce the photolytic degradation of TMP and NDEA.

H2: The presence/absence of the Fenton-mediated oxidation could serve as explanation of aerogels photoactivity.

# 1 LITERATURE REVIEW

## 1.1 Micropollutants – an invisible threat

Humanity has faced new problems related to the final treatment of the goods manufactured from the beginning of the industrial revolution. Micropollutants (MPs) are anthropogenic chemicals occurring in the environment above a natural background level due to human activities. Their concentrations remain at low levels – up to microgram per litre. A lot of chemicals are in this category – purely synthetic chemicals, like strongly halogenated molecules (fluorinated surfactants), or natural compounds like antibiotics (penicillins) or steroid hormones. These chemicals can originate from various sources (Figure 1) – agriculture, households, traffic networks or industries. (Stamm et al., 2016)

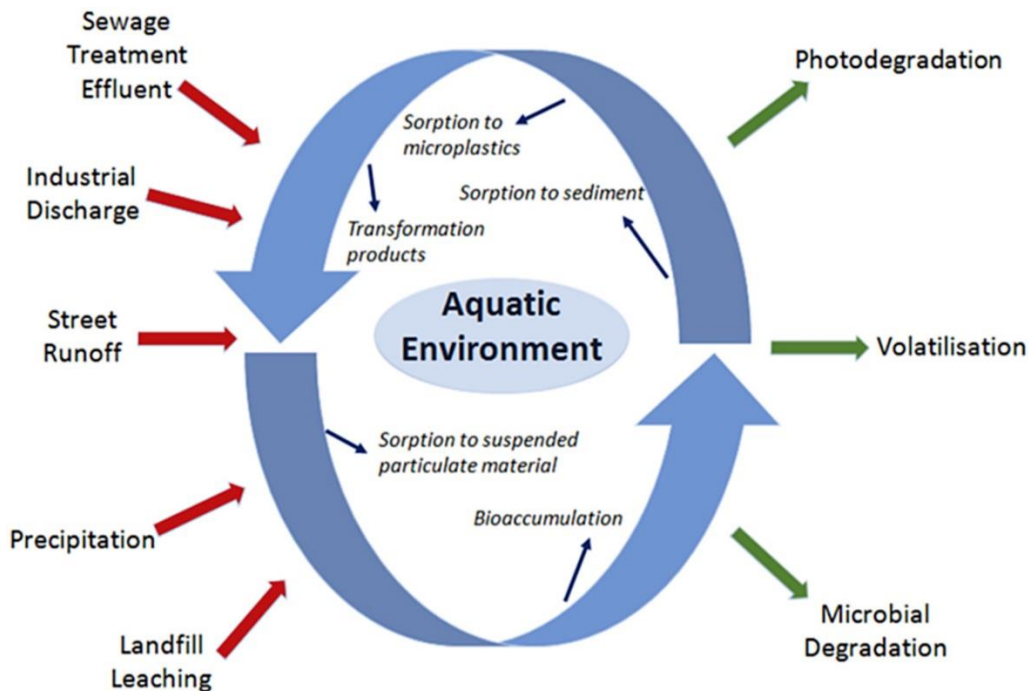


Figure 1. Sources and fates of micropollutants in aquatic environments (Wilkinson et al., 2017)

MPs enter aqueous systems by diverse entry paths, e.g. through diffusion or as a point source pollution (Stamm et al., 2016). Micropollutants have a negative impact on the quality of the environment and living organisms. Different processes occur in a water body, which is contaminated with organic matter. The water becomes depleted of oxygen which leads to eutrophication. Living organisms undergo bioaccumulation of pollutants, which can endanger life of these organisms. As a result, humans receive

hazardous pollutants by consumption of marine organisms from contaminated water bodies.

One of the most important humanitarian priorities is the secure access to clean drinking water. Unfortunately, almost half of the world's population has been living in water-stressed areas which has become a global problem in the twenty-first century. Although the use of chlorine in drinking water treatment has a positive impact on the water quality reducing the spread of waterborne pathogens. The chlorination of water could lead to the development of dangerous disinfection by-products (DBPs) by reactions between organic precursors and disinfectants (chlorine, chlorine dioxide, chloramines and ozone). This effect is considered as a significant disadvantage of chlorine disinfection (Bond, Templeton & Graham, 2012).

N-nitrosamines belong to a class of chemical compounds with molecular structure containing nitroso functional group (WHO, 2021). They are a type of emerging disinfection byproducts that reach the environment, as well as their precursors, via various sources, for instance recycled water, industrial byproducts, and domestic discharge. N-nitrosamines are known for their carcinogenic properties and therefore their presence in drinking water needs severe regulation in order to protect public health. The formation potential of N-nitrosamines in chloramination is mostly dependent on the occurrence of their precursors (Chen et al., 2021). Precursors include organic matter, anthropogenic contaminants (like detergents, industrial chemicals, dyes, pesticides and pharmaceuticals), brominated and iodinated compounds (Gilca et al., 2020). Therefore, any wastewater could serve as a source of N-nitrosamines precursors (Bond, Templeton & Graham, 2012). N-nitrosamines are formed during wastewater and drinking water disinfection processes, including chlorination, chloramination, and ozonation. N-nitrosodimethylamine (NDMA) formation undoubtedly has strong correlation with chloramination process. In addition, N-nitrosopyrrolidine (NPYR), N-nitrosomorpholine (NMOR), N-nitrosodiethylamine (NDEA), N-nitrosodiphenylamine (NDPhA) and N-nitrosodibutylamine (NDBA) occur in raw or treated drinking water. (Bond, Templeton & Graham, 2012)

N-nitrosamines intake has been linked with the increasing risk of cancer (Chen et al., 2021). By this reason, N-Nitrosodiethylamine is used in experimental research to induce liver tumorigenesis (National Center..., 2021a). Because of their carcinogenic abilities, N-nitrosamines should be carefully removed from drinking water before personal consumption, as well as from contaminated water, that is discharged to water bodies.

Pharmaceuticals, which are intended to be biologically active substances, are usually lipophilic and resistant to biodegradation, giving them the background for environmental accumulation and persistence (Klavariotia et al., 2009). A foreseen result of antibiotics presence in environment is antibiotic resistance of microorganisms, which remains a subject of growing concern nowadays. For instance, *Stenotrophomonas maltophilia*, a non-fermenting gram-negative bacterium, is one of the multidrug-resistant bacteria in hospital facilities (Brooke, 2014). Field study (Wu et al., 2021) in Taiwan medical center showed that in 10.6% of cases *S. maltophilia* strain was resistant to levofloxacin and combination of trimethoprim/sulfamethoxazole. This academic study suggests that the occurrence of high-level resistant strains of *S. maltophilia* may be limited by cautious use of fluoroquinolone and trimethoprim/sulfamethoxazole (TMP/SMX). (Wu et al., 2021)

However, TMP/SMX combination is included into WHO Model Lists of Essential Medicines and is properly considered to be first choice for lower urinary tract infections and second choice for acute invasive diarrhoea and bacterial dysentery (WHO, 2019). Into the bargain, it is discovered that treatment with TMP/SMX for *Pneumocystis* pneumonia improves lung function in pediatric asthma (Eddens et al., 2021). Similar combination – TMP and sulfadiazine is traditionally used in effective treatment of such domestic animals as calves, sheep, goats, poultry, and swine against many gram-positive and gram-negative bacteria like *E. coli*, *Haemophilus*, *Pasteurella*, *Salmonella*, *Staphylococcus* and *Streptococcus spp.* (Interchemie Werken «DE Adelaar» B.V., 2021). TMP is additionally used in the specific treatment of pneumonia and toxoplasmosis infections (Arti et al., 2021).

From the above information, it follows that trimethoprim is and will be widely used for the treatment of various diseases in humans and animals. As an undesirable result, the further entering of trimethoprim into the aquatic environment should be reasonably expected. It is suggested that in order to prevent antibiotic resistance, 1 µg/L would be a reasonable permissible exposure limit for trimethoprim in aquatic environments (Kraupner et al., 2020). However, the world research (University of York, 2019) finds, that most of the rivers are already contaminated with antibiotics above suggested level and trimethoprim is the most prevalent.

## 1.2 NDEA and TMP as study objects

N-Nitrosodiethylamine (NDEA) (Figure 2, Table 1) is a synthetic compound, which is light-sensitive, volatile, oily liquid of clear yellowish color. NDEA is soluble in water, lipids, and other organic solvents. (National Center for Biotechnology Information, 2021a).



Figure 2. Molecular structure of NDEA (National Center for Biotechnology Information, 2021a)

Table 1. Properties of NDEA (National Center for Biotechnology Information, 2021a)

Molecular formula	C <sub>4</sub> H <sub>10</sub> N <sub>2</sub> O
Molecular weight	102.14 g/mol
Solubility in water at 24 °C	106 mg/L
Boiling point	175-177 °C

NDEA has a variety of implementations on industrial scale, for instance as antioxidant, gasoline and lubricant additive, and stabilizer for industry materials, such as plastics. In process of heating to decomposition, N-nitrosodiethylamine emits toxic nitrogen oxides. It is considered to be a mutagen, which affects DNA integrity, a hepatotoxic and a carcinogenic agent. (National Center..., 2021a) Diethylamine is a precursor for N-nitrosodimethylamine and N-nitrosodiethylamine formation (Figure 3) (Kodamatani, et al., 2021).

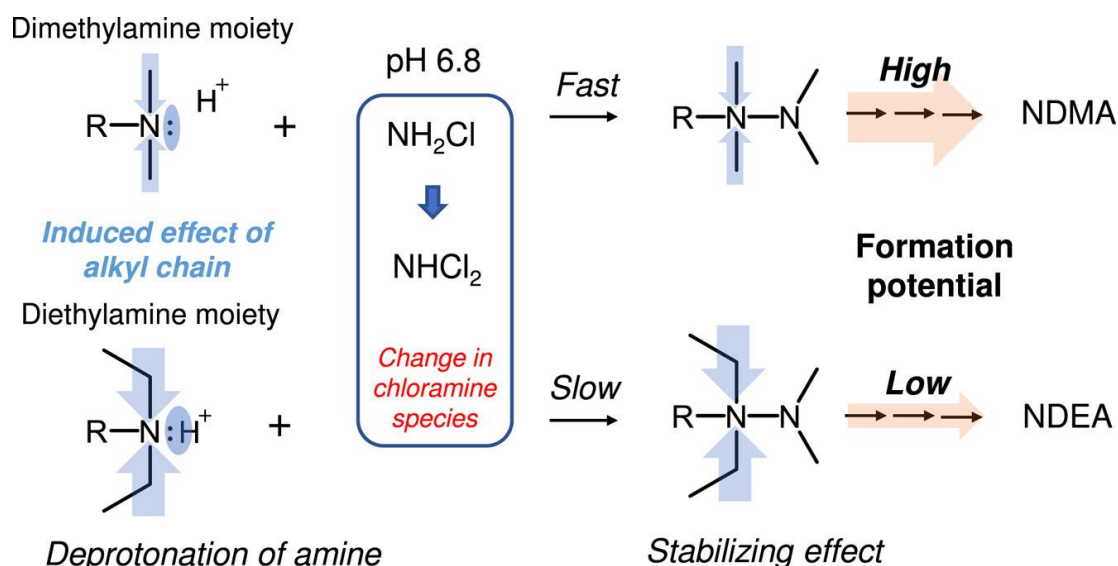


Figure 3. Formation mechanism of NDMA and NDEA as a result of chloramination (Kodamatani et al., 2021)

Figure 3 illustrates that the formation potential of N-Nitrosodiethylamine is lower than that of N-nitrosodimethylamine. Degradation of NDMA was intensively studied during last decades, but degradation of NDEA seem to be less studied, or studied in combination with NDMA. For instance, degradation of NDMA was studied using vacuum ultraviolet irradiation. Results show that removal of NDMA was successful with ultraviolet irradiation. (Fujioka et al., 2021) During other study, photolysis was also considered to be successful for removal of NDMA, however, results show that it did not affect concentrations of precursors of NDMA (Reny et al., 2021). Current study is willing to fill this gap in knowledge about degradation of NDEA to some extent.

Trimethoprim (Figure 4, Table 2) is an odorless white to cream crystalline powder with bitter taste. TMP is very slightly soluble in water and slightly soluble in alcohol (National Center for Biotechnology Information, 2021b). Synthetic bacteriostatic agent trimethoprim is designed to prevent production of the bacterial enzyme - dihydrofolate reductase (Arti et al., 2021). This enzyme participates in the synthesis of nitrogenous bases vital for the replication of bacterial nucleic acids (National Center..., 2021b). TMP was firstly applied for human infection treatment in 1962. In 1968 its combinations with sulfonamides were registered for clinical use. (Eliopoulos & Huovinen, 2001)

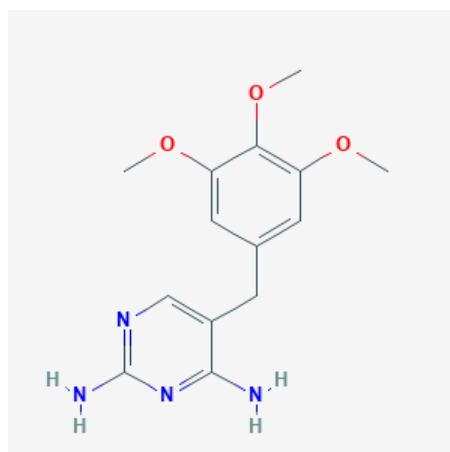


Figure 4. Molecular structure of TMP (National Center for Biotechnology Information, 2021b)

Table 2. Properties of TMP (National Center for Biotechnology Information, 2021b)

Molecular formula	C <sub>14</sub> H <sub>18</sub> N <sub>4</sub> O <sub>3</sub>
Molecular weight	290.32 g/mol
Solubility in water at 25 °C	400 mg/L
Melting Point	199-203 °C

Amine-containing pharmaceuticals were also reported to be precursors for nitrosamines formation during chlorination disinfection (Chen, Wang & Hsu, 2021), so examining methods for degradation of these both groups' presenters could benefit in finding complex solution to this problem.

### 1.3 Advanced oxidation processes in wastewater treatment

Wastewater treatment methods that are based on biological processes do not effectively remove organic micropollutants present in municipal wastewater. After technological purification recalcitrant organic pollutants generally remain unoxidized and possess toxic properties. Therefore, a need for the development of technology, in order to remove these toxicants from wastewater before discharging into water bodies, is of great importance.

Advanced oxidation processes (AOPs) can be the key to fill this need. In general, advanced oxidation processes can be defined as treatment processes, where driving force is hydroxyl radicals. Produced hydroxyl radicals oxidize organic pollutants, which results in purification of treated media. Hydroxyl radicals are nonselective and highly reactive electrophiles (Iervolino, Vaiano & Palma, 2020). Suitable physical conditions to apply this processes are close to ambient temperature and pressure. Exist a huge variety of different advanced oxidation processes, which can be divided into five groups (Figure 5). Advanced oxidation processes are used for treatment of liquids, gases and soil.

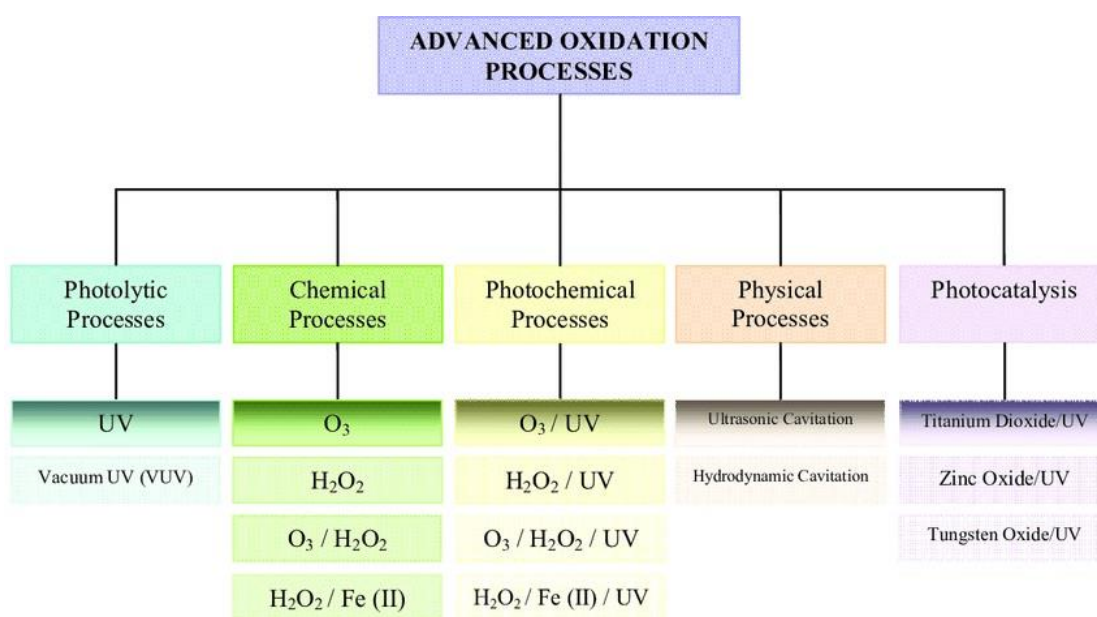


Figure 5. Classification of advanced oxidation processes (Chirwa & Bamuza-Pemu, 2010)

### 1.3.1 Photolytic processes

Photolytic processes are based on the absorption of UV radiation, which initiates pollutant degradation through direct or indirect photolysis. It is possible to use natural UV radiation or produce it from artificial sources. The energy produced by absorbed photons stimulates the activation of reactant molecules, which facilitates degradation reactions (Parsons & Williams, 2004). Direct photolysis is proceeded through absorption of UV light by organic compounds, which either helps them to react with water constituents or causes self-decomposition. The photodegradation of organic compounds induced by oxygen and hydroxyl or peroxide radicals formed by the photolysis of humic and inorganic substances is known as indirect photolysis (Chirwa & Bamuza-Pemu, 2010). UV and vacuum UV (VUV) photolysis cannot be used as stand-alone methods to

treat organic contaminants because of the creation of potentially dangerous byproducts (Buchanan, Roddick & Porter, 2006).

### 1.3.2 Chemical processes

Chemical processes are the oldest advanced oxidation processes used for degradation of organic pollutants. This category includes ozonation and hydrogen peroxide (H<sub>2</sub>O<sub>2</sub>) systems. Hybrid chemical systems combine these oxidants for pollutant degradation. These systems were developed to increase the degradation efficiencies of conventional chemical processes. The peroxone (O<sub>3</sub>/H<sub>2</sub>O<sub>2</sub>) and the Fenton reaction are two hybrid chemical-based systems commonly used for pollutant degradation in aqueous systems. Due to accelerated hydroxyl radical generation mechanisms, these systems have demonstrated higher efficiencies (Chirwa & Bamuza-Pemu, 2010). Below is a brief overview of the chemical systems, outlining their main benefits and disadvantages.

**Ozonation** mechanism is described in following reactions (Equations 1-6) (Chirwa & Bamuza-Pemu, 2010):



Ozone is a highly reactive gas that has a limited solubility in water (Shin et al., 1999; Zhou & Smith, 2002). Contaminant destruction by ozone occurs through a direct reaction of ozone with dissolved organic matter. This reaction is selective and needs a high electronic density. Another reaction happens between produced hydroxyl radicals and dissolved contaminants, this one is non selective. (Shin et al., 1999) Ozonation is more effective at degrading highly unsaturated compounds like alkenes, alkynes, and amines. Unfortunately, oxidation of aliphatic carbon chains, amides, and nitroso compounds by ozone is not so effective. Ozonation is combined with UV or H<sub>2</sub>O<sub>2</sub> in aim of boosting oxidation of O<sub>3</sub>-resistant contaminants, this increases the synthesis of hydroxyl radicals by speeding up the decomposition of ozone (Beltrán, Rivas & Montero-de-Espinosa, 2002; Lee, Yoon & von Gunten, 2007; Rosal et al., 2009).

One of the most significant disadvantages of ozone as an oxidant is its poor water solubility. Another factor is the expense of producing enough ozone for complete oxidation of organic compounds. Ozonation is limited by mass transfer (Shin et al., 1999). Bromide ions in water are converted to bromate ions by ozone, which poses some risks of using ozonation as disinfectant for drinking water treatment (Zhou & Smith, 2002; Michalski, 2003). In spite of disadvantages, ozonation is actively studied field and this process is widely used in water treatment.

**Hydrogen peroxide** is a relatively strong oxidant. It has limited use for the degradation of complex organic contaminants on its own because of kinetic limitations at acceptable concentrations. Combining H<sub>2</sub>O<sub>2</sub> with ozone, UV radiation or transition metal salts (for example Fe(II)) will improve hydrogen peroxide oxidative ability. Since H<sub>2</sub>O<sub>2</sub> is decomposed to release hydroxyl radicals, hybrid chemical systems have stronger oxidative properties. (Chirwa & Bamuzza-Pemu, 2010)

**Peroxone systems (O<sub>3</sub>/H<sub>2</sub>O<sub>2</sub>)** produce hydroxyl radicals (equation 7) through a radical chain mechanism (Chirwa & Bamuzza-Pemu, 2010).



The combination of O<sub>3</sub>/H<sub>2</sub>O<sub>2</sub> have better odds of complete mineralization of both the target pollutant and degradation byproducts (Rosal et al., 2009). The addition of a UV radiation source to the peroxone system will increase its performance even further (Chirwa & Bamuzza-Pemu, 2010). For extremely polluted effluents, it is thought as being the most effective treatment (Munter, 2001)

**The Fenton reaction** is named after British scientist Henry Fenton, who discovered in 1894 the ability of certain metals to have specific features of electron transfer (Fenton, 1894). The Fenton reaction mechanism (Equations 8-11) is described as the reaction between Fe(II) and H<sub>2</sub>O<sub>2</sub>, in role of the catalyst and oxidant, respectively, which results in generating Fe(III) and hydroxyl radicals (•OH) (Barb et al., 1951):



The rate-limiting step in this catalytic iron cycle is the regeneration of Fe(II) from Fe(III) (Oller & Malato, 2021). Another limitations of the traditional Fenton process are:

- iron containing sludge production;
- pH range;
- active components separation from the reaction solution. (Zhu et al., 2021)

The Fenton process is largely used in treatment of organic contaminants in soil and water. Fe(II) can be replaced by Fenton-like reagents, such as Cu(I), Cr(II), CO(II) and Ti(III), which have similar oxidative features to the Fenton reagent (Chirwa & Bamuza-Pemu, 2010).

### 1.3.3 Photochemical processes

Photochemical processes combine chemical oxidants with UV radiation, which accelerates hydroxyl radicals' production. The O<sub>3</sub>/UV system, the H<sub>2</sub>O<sub>2</sub>/UV system, the O<sub>3</sub>/H<sub>2</sub>O<sub>2</sub>/UV system, and the photo-Fenton (Fe(II)/H<sub>2</sub>O<sub>2</sub>/UV) system are all photochemical processes.

**Photo-Fenton.** In presence of light, Fenton reactions are accelerated, regenerating Fe(II) and producing more •OH (Oller & Malato, 2021). Acceleration of the Fenton process by light is named the photo-Fenton process. The photo-Fenton process occurs at  $\lambda < 580$  nm, thus solar energy can be applied as a green energy source (Oller & Malato, 2021). The complexes in the Fenton reaction absorb light, as a result, generation of •OH is increased. The optimum reaction pH is 2.8, because in acidic media precipitation of iron is avoided. Furthermore, maximum amount of active iron species (FeOH<sup>+</sup> and Fe(OH)<sub>2</sub><sup>+</sup>) are present at this pH. (Oller & Malato, 2021) In recent study (Saleh et al., 2021) the photo-Fenton process efficiency was compared to the classical Fenton for dye removal with basalt powder used as catalyst. The Fenton process removed 87% of methylene blue and 28% of basic red 18. For methylene blue, the photo-Fenton process had a 100% removal efficiency, and for basic red 18 dye, it had a 70% removal efficiency. (Saleh et al., 2021)

### 1.3.4 Physical processes

Physical processes such as cavitation can also serve as sources of hydroxyl radicals production. During the cavitation process the sequence of compression and rarefaction

cycles creates the cavitation bubbles in liquid phase. Extremely high pressure (around 50 atm) followed by implosion of cavitation bubble produces adiabatic heating, where temperature could increase up to 5000 K. Such physical conditions instigate the formation of hydroxyl radicals, which promote oxidation of pollutants. Thus, two mechanisms of cavitation – pyrolysis and hydroxyl radicals attack provide the oxidation of contaminants. Among the disadvantages of such treatment is a high energy consumption and concomitant metal corrosion, which can limit applications of this process for water treatment. Ultrasonic waves and hydraulic devices can cause cavitation in a liquid as well. Ultrasonic cavitation can also be called acoustic cavitation. In this treatment method high frequency sound waves incept cavitation in liquid. Hydrodynamic cavitation is induced by hydraulic devices. In this systems pressure variations in flowing liquids generate cavitation by change in the shape of system. Membranes and valves cause pressure variations in liquid passing through. On one hand acoustic cavitation intensity is higher than that of hydrodynamic cavitation. But on the other hand, cavitation yields and efficiency of hydrodynamic cavitation is higher compared to acoustic cavitation. (Chirwa & Bamuzza-Pemu, 2010)

### **1.3.5 Photocatalytic processes**

Photocatalytic reactions are common in nature – for example, photosynthesis. Photocatalysis is the process of accelerated chemical reactions in the presence of a catalyst and light radiation. Light-reactive substances enter an excited state, which allows them to interact effectively with the catalyst - the reaction takes place only under the influence of light on the surface of the catalyst. (Chirwa & Bamuzza-Pemu, 2010)

Semiconductor photocatalysis is the process of a solid semiconductor activation during electromagnetic radiation absorption, usually in the near ultraviolet range of light spectrum. Semiconductor materials usually have electronic structures that consist of a valence band and a conductance band. In the valence band, occupied electrons reach the highest level, and in conductance band – the lowest. This bands are separated by regions that are free from energy levels. The band gap energy ( $E_{bg}$ ) is the difference in energy between two bands. As a result of photons ( $h\nu$ ) adsorption activated photocatalyst promotes an electron ( $e^-$ ) from valence band to conductance band, which generates a hole ( $h^+$ ) in the valence band. So, the electron-hole pair ( $h^+ e^-$ ) is formed (Figure 6). (Chirwa & Bamuzza-Pemu, 2010)

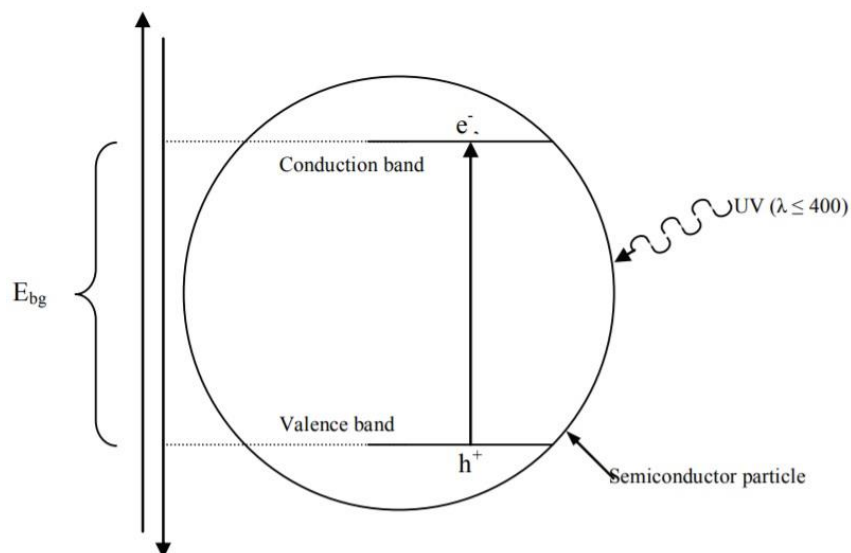


Figure 6. Electron-hole pair formation over a semiconductor particle (Chirwa & Bamuzza-Pemu, 2010)

Conductance band holes and electrons in excited state are able to:

- get captured in a metastable surface state;
- recombine inside or at the surface of the semiconductor material, scatter the energy as heat ( $\Delta$ );
- create separate ways to the semiconductor material's surface, where directly or indirectly reacting with adsorbed on the surface electron donors and acceptors, or within the charged particles' electrical double layer. (Chirwa & Bamuzza-Pemu, 2010)

In the absence of electron hole scavenger, recombination causes the dissipation of the energy stored. In the presence of electron scavenger or availability of surface defect state to catch the electron or hole and prevent recombination redox reactions can occur. (Hoffmann et al., 1995)

Oxidation potential of valence band holes varies between +1.0 and +3.5 V, making them powerful oxidants (Hoffmann et al., 1995; Munter, 2001). Electron hole pairs react with electron acceptors or electron donors adsorbed on the surface of photocatalyst. From electron acceptor (A) is produced a reduced product ( $A^-$ ), from electron donor (D) – an oxidised product ( $D^+$ ) (Figure 7, Equation 12). (Chirwa & Bamuzza-Pemu, 2010)



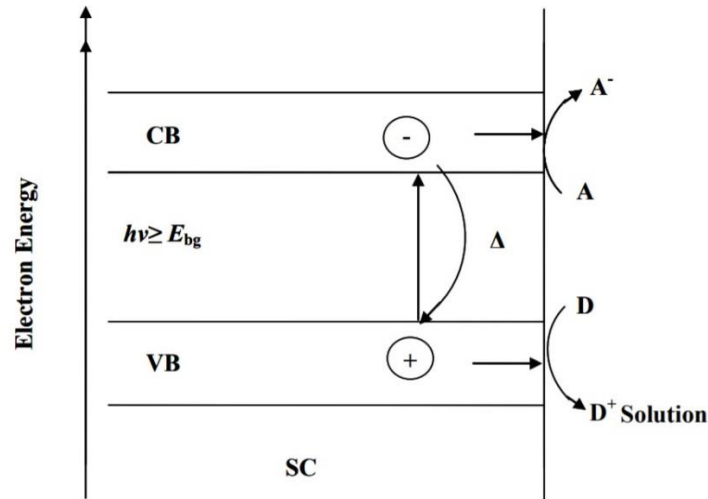
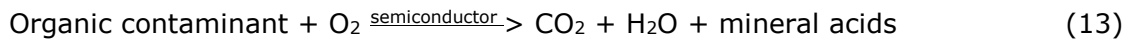


Figure 7. Energetics of semiconductor photocatalysis, where CB - conductance band, VB - valence band, SC - semiconductor (Chirwa & Bamuzi-Pemu, 2010)

In water treatment, oxygen serves as the electron acceptor (A) and the contaminants are the electron donors (D), so the process of photocatalytic oxidation of contaminants can be described by Equation 13. (Chirwa & Bamuzi-Pemu, 2010)



The most known photocatalysts are (Hoffmann et al., 1995; Li et al., 2015; Deng et al., 2021):

- cadmium selenide (CdSe);
- cadmium sulphide (CdS);
- ceric dioxide (CeO<sub>2</sub>);
- ferric oxide (Fe<sub>2</sub>O<sub>3</sub>);
- molybdenum disulphide (MoS<sub>2</sub>);
- molybdenum trioxide (MoO<sub>3</sub>);
- stannic dioxide (SnO<sub>2</sub>);
- titanium dioxide (TiO<sub>2</sub>);
- tungsten disulphide (WS<sub>2</sub>);
- tungsten trioxide (WO<sub>3</sub>);
- zinc oxide (ZnO);
- zinc sulphide (ZnS);
- zirconium dioxide (ZrO<sub>2</sub>).

Photocatalytic processes can be successfully applied in environmental technologies. These processes may serve as an excellent tool for removing of micropollutants. In addition, they possess less selectivity than ozonation (Kwarciak-Kozłowska, 2019). Photocatalytic technologies show promising results in degrading diesel fuel from seawater at a high rate (Nazri & Sapawe, 2020). Recently, the effect of photocatalytic processes on pollutant degradation in wastewater treatment has been extensively studied (Klavariotia et al., 2009). Photocatalytic oxidation is known for an excellent purification of wastewater containing pharmaceuticals and other organic pollutants (Deng et al., 2020).

The photocatalytic method has the advantage in terms of low economic costs compared to other methods, for instance, ozonation (Zhu & Wang, 2017). Moreover, this method is simple in operation, does not require expensive equipment and has high treatment efficacy (Choi et al., 2017; Luo et al., 2019). Photocatalytic oxidation can be conducted in slurry reactors or in fixed-catalyst reactors (Espíndola et al., 2019; Das & Mahalingam, 2020). In addition, photocatalysis can become the tool for green chemistry in wastewater treatment. Ecological photocatalytic ZnO nanoconjugates based on thiol ligands can be reused for up to 80% (Borsagli & Paiva, 2021).

Therefore, this method is chosen for the treatment of water containing organic micropollutants. Metal doped aerogels could highly likely possess photocatalytic properties (Bolobajev et al., 2019). So, this material was subjected for the present study.

## 1.4 Aerogels

The successful inventor of aerogels is Samuel Stephens Kistler, who firstly synthesized aerogels in 1929-1930 (Kistler, 1931; Kistler, 1932). According to Alemán et al. (2007) aerogels can be defined as gels comprised of a microporous solid material in which a gas is present in a dispersed phase. However, not only micropores with diameter less than 2 nm, but also mesopores (2-50 nm) and macropores (50 nm) could be present in aerogels (Jiang et al., 2021). Aerogels are open-cell, three-dimensional assemblies of organic or inorganic nanoparticles (Figure 8) (Chandrasekaran & Adarsh, 2021).

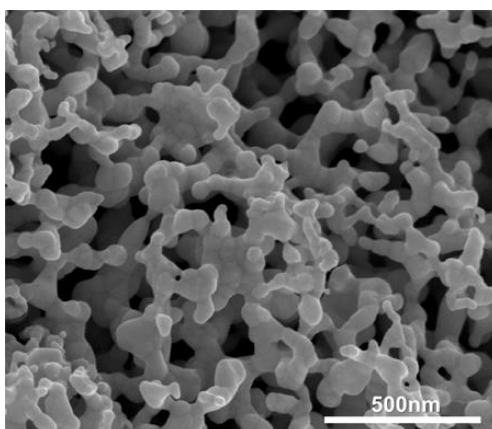


Figure 8. 3D structure of gold aerogels (Burpo et al., 2017)

The unique feature of aerogels is that these materials retain nanoscale properties in macroscale (Jiang et al., 2021). Aerogels are undoubtedly known for their low density, open porosity, and large surface area (Manzocco, Mikkonen & García-González, 2021). One of the most known aerogels are silica aerogels, which is now produced on an industrial scale. Today, leading producers of aerogels are Aspen Aerogels, Aerogel Technologies, American Aerogel, BASF and Cabot (Maida, 2021).

Aerogels can be grouped into 2 large groups - single-component and composite aerogels, which can be further divided into following groups according to their composition (Jiang et al., 2021):

- carbon aerogels;
- cellulose aerogels;
- metal aerogels;
- organic aerogels;
- oxide aerogels;
- polyurethane aerogels;
- resorcinol formaldehyde aerogels (Erkhova et al., 2020);
- etc.

One of the methods to produce aerogels is to obtain solid structure from gels. Term gel here refers to colloid in which a liquid is dispersed in a solid. Gels can be made by gelation process, when solution containing precursors is prepared and the solid network is synthesized from precursors. The formation of resultant colloid influences the properties and the structure of subsequent aerogel. For example, polymer chains provide mechanical flexibility. Three groups can be determined depending on precursors:

- polymer aerogels;
- molecular aerogels;
- colloidal aerogels. (Jiang et al., 2021)

To produce polymer aerogels the first step is to prepare polymers from polymerizing monomers. Then polymers are linked to wet gels and dried forming aerogels. For molecular aerogels molecular gelators solution is firstly mildly heated then cooled forming wet gels. Final step is drying to obtain aerogels. Production of colloidal aerogels starts with precursor solution conversion to colloidal sols (here liquid with dispersed solid phase in it), then wet gel is formed from colloidal particles and dried. (Bheekhun, Talib & Hassan, 2013; Jiang et al., 2021)

Using common evaporation for drying of gels results in producing xerogels, which pores are retained less. This is a result of large capillary forces development in the network of gels. For removing of liquid phase from gel it can be placed under supercritical conditions, where drying occurs without disrupting unique structure of gel (Bheekhun, Talib & Hassan, 2013). This process is named critical point drying (CPD) and alcohol is used as a solvent (ethanol or acetone).

Another possible option is freeze drying (FD) process, where water is commonly used as a solvent. Equipment requirements for this process are little, so it serve a certain interest. (Jiang et al., 2021) The liquid-gas phase boundary is bypassed in both processes, so fluctuation of the surface tension is avoided, and large specific surface areas can be obtained (Du et al., 2014). However, freeze drying efficacy is lower than that of critical point drying. Generated ice crystals and expanded water volume can damage microstructures during freezing. This problem can be eliminated by using of liquid nitrogen to provide instant freezing or some other solvent, e.g. tert-butanol.

Third possible option to obtain aerogels is ambient pressure drying (APD). This process is used for production of silica aerogels, because of its low costs and better suitability for manufacturing (Jiang et al., 2021) During this process, surface tension change is reduced by usage of solvents with low surface tension or by modification of gel with trimethylchlorosilane in a sake of surface energy reduction (Sarawade et al., 2007). In comparison with critical point drying and freeze drying, ambient pressure drying is less effective due to presence of impurities in final product. (Jiang et al., 2021)

There is a high amount of aerogels varieties, which could remarkably differ in terms of their properties and numerous possible applications. Due to low heat transfer property (Figure 9), silica aerogel-based materials are known to be used for thermal insulation in construction (Lamy-Mendes et al., 2021), pipelines, transportation, space vehicles and protective clothing, like firefighters' equipment (Mazrouei-Sebdani et al., 2021).

As it was hitherto mentioned, aerogels are used in spaceships construction as well. The most known example is spaceship Stardust. Silica-based aerogel is used to catch interstellar dust. Because of aerogel's high porosity, its application allows to catch active species without damaging them. This created an opportunity to analyze samples of interstellar dust (Grier & Rivkin, 2019).



Figure 9. Silica aerogel protects flower from heat of Bunsen burner (Condliffe, 2014)

Furthermore, aerogels have found the application in medicine. Some aerogels can be applied for prompt oral drug delivery (García-González et al., 2021). Negatively charged graphene oxide-gelatin aerogels show superior blood clotting performance (up to 95.6%), so these valuable materials can potentially be employed as a hemostatic device for bleeding wounds (Guajardo et al., 2021).

Also, aerogels show remarkable results in environmental technology. Aerogels are well-known for superior adsorption properties due to their unique structure that contains pores of different size (2-50 nm) (Jiang et al., 2021). Aerogels are profitably employed as an adsorbent to promptly remove volatile organic compounds from the air and are extensively considered for successful carbon dioxide capture (Maleki, 2016).

Recently conducted studies have shown great adsorption abilities of various aerogels for different aqueous solutions with organic contaminants. Aerogels are knowingly used for successful removal of the oil spill, toxic organic compounds and heavy metal ions from wastewaters (Maleki, 2016). For instance, cellulose aerogels demonstrate considerable potential in methylene blue removal from wastewater (Luo et al., 2021). Nanofiber aerogels efficiently absorb oil from wastewater (Wu et al., 2021). Chitin-psyllium based aerogels were tested to absorb crystal violet dye from aqueous solution, results show that these aerogels are possibly able to treat wastewaters with other dyes (Druzian et al., 2021). Silica aerogels are used in processes of absorption, filtration and separation in wastewater treatment (Mazrouei-Sebdani et al., 2021). In field study adsorption properties of silica aerogel towards presenter of different organics were studied, results

show rapid adsorption with capacities of 12.00 g/g for epoxy resin, 10.86 g/g for silicone oil, 10.23g/g for methanol, 9.83 g/g for ethanol and 6.48 g/g for hexane (Yao et al., 2021). Graphene oxide cadmium sulfide composite aerogels have shown superior adsorption ability in experiments with organic aqueous solutions of gasoline, paraffin liquid, pump oil, ethanol, cyclohexane, hexane, toluene and chloroform (Xu et al., 2021). Magnetic hydrophobic aerogels with Fe<sub>3</sub>O<sub>4</sub> nanoparticles had the adsorption rate of 181 g/g for silicone oil, 176 g/g for motor oil, 155 g/g for corn oil, 101 g/g for soybean oil and 118 g/g for pump oil, in addition showing great reusability (He et al., 2021). Iron-based metal-organic cellulose aerogels showed great ability to adsorb Congo red dye (Huang et al., 2021). In one study (Huang et al., 2021) graphene carbon aerogels showed adsorption capacities of 289–410 g/g for oil/water separation. Aerogels were obtained from graphene carbon nanotubes using waste polyethylene (Huang et al., 2021).

Having several advantageous traits, e.g. open porous structure, large surface area and the possibility of deposition of functional composites, aerogels contribute a plenty of scope for processes to occur including photocatalysis.

## 1.5 Metal aerogels

Metal aerogels are aerogels, which are doped with metals as a three-dimensional network of nanosized metal particles. This group of aerogels is quite new being firstly developed about 10 years ago. The first created metal aerogels were iron aerogels (Leventis et al., 2009) and noble metal aerogels (Bigall et al., 2009). Nowadays following elements can be successfully used for forming single-component metal aerogels:

- titanium;
- iron;
- cobalt;
- nickel;
- copper;
- ruthenium;
- rhodium;
- palladium;
- silver;
- tin;
- tantalum;
- osmium;
- platinum;
- gold. (Jiang et al., 2021)

Metal aerogels are usually prepared by gelation and drying, but freeze-casting can also be applied. Freeze-casting method combines gelation and drying in one step, which simplifies fabrication process and adds structure flexibility (Gao et al., 2014). Gelation methods are typically divided into one-step and two-step strategies. It depends on transformation of metal salts to gels: in one step strategy it occurs directly, but in two-step strategy metal nanoparticles are formed before gelation. Exist 6 important factors of synthesis process:

- initiator;
- precursor;
- reductant;
- ligand;
- solvent;
- external field. (Jiang et al., 2021)

The most explored factor is initiation, which determines the path of gels formation and influences the reaction time and material morphology (Jiang et al., 2021). Initiation methods are diverse, including pH control (Naskar et al., 2017), oxidant-triggered method, solvent introduction (Bigall et al., 2009), reductant-triggered method (Liu et al., 2013), salts as initiators (Wen et al., 2014), monovalent cations as initiators (Du et al., 2019) etc.

Precursors for metal aerogels include metal salts, metal nanobuilding precursors (for example, nanoparticles) and metal gels. Metal salts are used in one-step gelation method, providing easy fabrication possessing difficult morphology control, on another hand. Metal nano-building precursors are used in two-step method, allowing to control structure of metal aerogels, but this method is complicated and the control of morphology is limited. Metal gels as precursors allow to obtain perfect network connectivity and special morphologies, but this method is complicated, expensive and time consuming. (Jiang et al., 2021)

Reductants are needed to convert metals in the form of salt to zero-valence form. It is present a variety of applied reductant methods, which includes solid-solid reduction (for example, with carbon or magnesium) (Leventis et al., 2009; Chen et al., 2014), liquid phase reduction (e. g. with  $\text{NaBH}_4$ ) (Liu et al., 2013) and liquid-gas reduction (e. g. with carbon monoxide) (Yazdan-Abad et al., 2019). Implication of certain reductants can offer control over metal aerogels morphology.

Ligands chemistry is less explored in the metal aerogels synthesis. However, it is well studied in field of nanocrystals synthesis. Water is the most common solvent for gelation processes of metal aerogels (Jiang et al., 2021). The use of non-water solvents is a relatively new approach. Non-water solvents include 1-octadecene, hexane (Naskar et al., 2017) and carboxylic acids (Yazdan-Abad et al., 2019). In the current study dioxane was applied as a solvent, which widens this relatively young field of study.

External factors like temperature, magnetic force and light can also influence the gelation process and properties of obtained metal aerogels (Jiang et al., 2021). For example, in the current study, Sol-Gel process underwent at 60 °C using thermostat.

Metal aerogels combine properties of aerogels, such as low density, high porosity, self-supported network, light weight and large surface area with properties of alloyed metals, for example catalytic activity, electrical conductivity optical feature and plasticity (Jiang et al., 2021). This combination will make them useful as high-surface-area electrodes for example in supercapacitors, batteries, fuel cells and water desalination. Aerogels made of iron, cobalt and nickel, and may be the tool for energy conversion and storage devices. This would be useful for making effective and lightweight catalytic converters, which can result in shifting from expensive platinum group elements to cheaper iron and nickel aerogels. (Alwin & Shajan, 2020)

Metal nanoparticles have higher catalytic activity than the bulk forms of metals. For this reason, noble metal aerogels are attractive substances due to their large surface areas and catalytic properties (Du et al., 2020). For example, gold in the bulk form is not catalytic, while gold nanoparticles efficiently catalyze reactions, such as carbon monoxide oxidation to carbon dioxide in room-temperature conditions and the growth of carbon nanotubes (Vallribera & Molins, 2007; Du et al., 2020). The oxidation of carbon monoxide in presence of gold nanoparticles possibly solves CO pollution problem in transportation (Du et al., 2020). Also, gold aerogels can be successfully applied in electrocatalysis: electrodes modified with gold aerogels have high nonenzymatic glucose oxidation ability, which could lead to production of glucose sensors and fuel cells with high performance (Wen et al., 2016). Noble metal aerogels have demonstrated successful electrocatalytic performance in oxidation of methanol, ethanol, ethylene glycol and in reaction of oxygen evolution. In addition, noble metal nanoparticles can be applied in a liquid-phase heterogeneous catalysis, for instance in dye degradation. The degradation of dyes is important for treating industrial wastewater. The combination of Ag<sub>34</sub>Au<sub>33</sub>Pd<sub>33</sub> nanosponge with NaBH<sub>4</sub> can rapidly oxidize Congo red dye. (Du et al., 2020)

Metal aerogels show promising results in environmental technology. As it was hitherto mentioned, metal aerogels are suitable materials for electrocatalysis. Metal aerogels were applied in the CO<sub>2</sub>-RR electrocatalytic reaction, which is the conversion of carbon dioxide into high valued fuels. Recent study shows that bimetallic Pd-Cu aerogels are perfectly suitable for the performance of the CO<sub>2</sub>-RR reaction on their surface in 1-butyl-3-methylimidazolium tetrafluoroborate aqueous solution. (Lu et al., 2018) Metal aerogels can also be used for water purification. In case study (Tang et al., 2013) Cu nanowire aerogels were modified with (heptadecafluoro-1,1,2,2-tetradecyl) trimethoxysilane. As a result, were obtained superhydrophobic ultralight aerogels. Mentioned materials were able to adsorb spills of organic oil. On the other hand, metal aerogels containing toxic metal ions could not be the best choice for this procedure, because of secondary pollution of treated water. (Tang et al., 2013)

Metal oxide aerogels, were also successfully applied in environmental technology. Field study (Liao et al., 2021) was conducted to explore opportunity of removing uranium from wastewater using metal oxide aerogels. Study found that adsorption capacity of CeO<sub>2</sub>, Pr<sub>2</sub>O<sub>3</sub> and Nd<sub>2</sub>O<sub>3</sub> aerogels were higher than other adsorbents, reaching values of 481.5, 840.6 and 587.3 mg/g, respectively. Results indicate that examined metal oxide aerogels are able to remove U<sup>4+</sup> from nuclear wastewater. (Liao et al., 2021)

In another study by Huang et al. (2018) solid phase microextraction (SPME) fiber covered by metal organic frameworks have shown great performance in adsorption experiments with N-nitrosamines. Metal organic frameworks are three-dimensional materials consisting of organic molecules that hold metallic ions in place (Qin, Hao & Li, 2020). In study of Huang et al. (2018) metal organic frameworks contained the 8-aminocaprylic acid doped UIO-66 (building bricks made of Zr<sub>6</sub>O<sub>4</sub>(OH)<sub>4</sub> with struts of 1,4-benzodicycarboxylic acid). It should be mentioned that discussed metal organic frameworks were intentionally designed for N-nitrosoamine adsorption purpose considering the fact that addition of functional groups generally reduces special surface area, pore size and therefore adsorption capacity of the obtained material. To enhance adsorption of N-nitrosoamines Huang et al. (2018) invented modulator-induced defect-formation strategy using the 8-aminocaprylic acid as a modulator to introduce amino groups, which are polar to N-nitrosoamines into UIO-66. Designed material were able to adsorb N-nitrosodipropylamine, N-nitrosodibutylamine, N-nitrosodiphenylamine and N-nitrosodiethylamine. However, adsorption performance for NDEA was the weakest of explored chemicals. (Huang et al., 2018) Results of this study indicate that development of special design with intended purposes can benefit in great degradation result of studied substances.

In experimental study (Bolobajev, Kask & Koel, 2019) metal doped organic aerogels were successfully applied for the treatment of water contaminated with pharmaceuticals. Cobalt, copper, sodium, nickel, zinc and iron doped organic aerogels showed potential for removing of trimethoprim by adsorption and photocatalysis with the best result achieved with nickel doped organic aerogel. Another advantage of using this aerogels for photocatalytic water treatment is absence of secondary pollution of treated water with metal ions. (Bolobajev, Kask & Koel, 2019)

Ferrocene aerogels belong to resorcinol formaldehyde aerogels group. During experimental study (Erkhova et al., 2020) ferrocene was introduced into resorcinol formaldehyde polymer to obtain electrochemically active aerogels. Obtained aerogels were structurally similar to resorcinol formaldehyde aerogels, being amorphous substances. All iron atoms in those aerogels belong to ferrocene or ferrocenium in ratios varying in 60/40-55/45 gap. Ferrocene precursor conversion rate into aerogels were about ~6 wt%, which could be due to the presence of micro-level defects in the structure of initial polymer. Ferrocene aerogels are likely to show reversible redox activity in reaction with reagents in gaseous phase. (Erkhova et al., 2020)

Applying ferrocene aerogels in current study can widen their possible implications, e.g. in photochemistry or photocatalysis.

## 2 MATERIALS AND METHODS

### 2.1 Reagents and chemicals

N-nitrosodiethylamine ( $C_2H_6N_2O \geq 99.5\%$ ) and trimethoprim ( $C_{14}H_{18}N_4O_3, \geq 98\%$ ) were purchased from Ehrenstorfer and Acros Organics, respectively. O-phenathroline monohydrate ( $C_{12}H_{10}N_2O, \geq 99.5\%$ ), sulfuric acid ( $H_2SO_4, 96\%$ ) were purchased from Lach:Ner. Hydrogen peroxide ( $H_2O_2, \geq 30\%$  w/w), acetic acid glacial ( $CH_3COOH, \geq 99\%$ ), ammonium acetate ( $CH_3COONH_4, \geq 98\%$ ), ferrous sulphate heptahydrate ( $FeSO_4 \cdot 7H_2O, \geq 98\%$ ), hydroxylamine hydrochloride ( $NH_2OH \cdot HCl, \geq 99\%$ ), 1,4-dioxane anhydrous ( $C_4H_8O_2, \geq 99.8\%$ ), formaldehyde solution ( $HCHO, 37\%$  w/w) were purchased from Sigma-Aldrich. All other reagents (potassium ferrioxalate, sodium sulphite, 5-methylresorcinol) were of analytical grade at greater than 95% purity used without further purification.

All solutions were prepared using ultrapure water obtained from a Millipore ultrapure water UV-system (Simplicity®, EMD Millipore Corporation, Billerica, MA, USA).

### 2.2 Experimental setup of photo-induced degradation of pollutants

For photolysis and photo-induced experiments with ferrocene and iron-doped organic aerogels 1 L glass cylindrical batch mixing reactor (Figure 10) with the UV lamp coated with a quartz tube was chosen. This reactor was used to treat water contaminated with N-nitrosodiethylamine and trimethoprim. To perform photolysis laboratory tests contaminant solutions were irradiated. In case of photo-induced degradation laboratory tests the powdered catalyst (aerogel concentration = 10 mg/L) was suspended in a contaminant solution and mixture was irradiated.

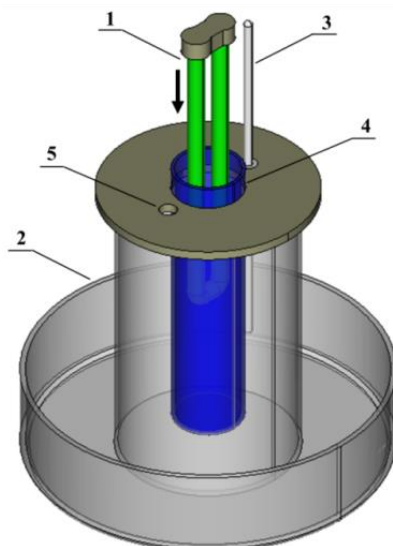


Figure 10. 3D model of the batch photo-reactor. 1 - UV lamp; 2 - external cooling jacket; 3 - thermometer; 4 - quartz tube; 5 - sampling port (Kask, 2017)

Initial concentrations of N-nitrosodiethylamine and trimethoprim in separate contaminant solutions were 10  $\mu\text{M}$ . The pollutant solution ( $V = 800 \text{ mL}$ ) is poured into a cylindrical batch mixing reactor equipped with the UV-A (OSRAM, DULUX® S BL, with capacity of 11W) or the UV-C lamp (Philips TUV PL-S, with capacity of 11 W) and a thermometer to monitor the change in temperature of the solution as a result of irradiation during the test. To maintain a constant temperature ( $22 \pm 2 \text{ }^\circ\text{C}$ ), a water jacket was used for cooling the studied solution. At the beginning of the test, the catalyst is suspended in contaminated water and the lamp is switched on. Sample ( $V = 3 \text{ mL}$ ) withdrawal was accomplished at predetermined time intervals (0, 5, 10, 15, 30, 45, 60, 90 and 120 min) using pipet.

All samples with TMP were filtered using a polytetrafluoroethylene (PTFE) filter (VWR International, 25 mm syringe filter, 0.45  $\mu\text{M}$  pore size) in order to separate aerogel from liquid phase. This filter was chosen, because it does not adsorb TMP. For experiments with N-nitrosodiethylamine a cellulose acetate (CA) filter (MACHEREY-NAGEL GmbH & Co. KG, 25 mm syringe filter, 0.45  $\mu\text{M}$  pore size) was used.

## 2.3 Fenton reaction experiments

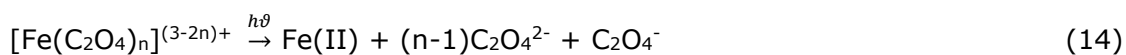
The Fenton oxidation of studied pollutants was conducted in batch cylindrical reactors at ambient temperature ( $22 \pm 1 \text{ }^\circ\text{C}$ ) and under acidic conditions (pH 3.0). For pH

measurement digital Mettler Toledo pH-meter S220 was used. The initial concentration of H<sub>2</sub>O<sub>2</sub> was 100 μM. The oxidation process was initiated by simultaneous addition of 10 μM of Fe(II), or ferrocene aerogel, or iron-doped organic aerogel and H<sub>2</sub>O<sub>2</sub>. The reaction mixture was mixed continuously using a multiple magnetic stirrer. Oxidation was stopped by 0.1 M Na<sub>2</sub>SO<sub>3</sub> solution addition (V = 0.5 mL). Sample withdrawal was accomplished at predetermined time intervals (0, 1, 2, 3, 4, 5, 10, 15 min for experiments with Fe(II) and 0, 3, 5, 10, 15, 30, 45, 60 min for experiments with ferrocene and iron-doped organic aerogels) using pipet. Test samples with aerogels were filtered with PTFE filter in case of TMP test solution and CA filter in case of NDEA test solution.

## 2.4 Determination of a quantum yield

Actinometer is defined as „chemical system for the determination of the number of photons integrally or per time interval absorbed into the defined space of a chemical reactor“ (Braslavsky, 2007). Actinometry was used to determine quantum yield of compound’s photolysis and photo-induced degradation. The quantum yield, Φ is the “number of defined events occurring per photon absorbed by the system” (Braslavsky, 2007). In photochemistry it is the difference between numbers of converted or formed molecules and absorbed photons in a period of time (Roibu et al., 2018).

Actinometry experiments were performed using a chemical actinometer, 0.006 M potassium ferrioxalate solution. The potassium ferrioxalate actinometer working principle is based on the reaction between the [Fe(C<sub>2</sub>O<sub>4</sub>)<sub>n</sub>]<sup>(3-2n)+</sup> complex and light photons (photodecomposition), which takes place in water (Equations 14 & 15) (Demas et al., 1981).



In order to avoid the influence of ambient light on the actinometry, all the experiment procedures were performed in a dark room and the solution of ferrioxalate was stored in a nontransparent box. Formed under UV irradiation iron moles were measured photometrically at λ = 492 nm using o-phenanthroline method. Absolute quantum yield of Fe(II) at 253.7 nm is generally accepted as 1.25 mol/E. (Bolobajev et al., 2019)

## 2.5 Analysis equipment and methods

Test samples with contaminated water were analyzed for the presence of either TMP or NDEA. The concentrations were determined using a high performance liquid chromatography (HPLC) equipment (YL-Instrument 9300, Young Lin Instrument Corporation, Hogye-dong, Anyang, Korea) equipped with a Waters Bridge (150 mm × 3.0 mm inner diameter) C18 (3.5 μm particle size) column and UV/Vis detector with deuterium lamp as a light source.

For N-nitrosodiethylamine isocratic elution was applied. The mobile phase was a mixture of 80% eluent A (0.1% acetic acid in ultrapure water), and 20% eluent B (pure acetonitrile) at the flow rate of 0.2 mL min<sup>-1</sup>. Detection was performed at 230 nm. The total analysis time was 13 min. The injected sample volume was 20 μL.

For the determination of trimethoprim, a gradient elution was applied using eluent A (0.1% acetic acid in ultrapure water) and B (pure acetonitrile). The total flow rate was 0.2 mL min<sup>-1</sup>. Elution started with 100% of eluent A (0.1% acetic acid in ultrapure water) with the subsequent decrease to 20% during 10 minutes with 5 min holdup. Then the concentration of eluent A rose up to 100% and continued at this eluent composition until 30 min. Detection was performed at 270 nm. The total analysis time was 30 min. The injected sample volume was 20 μL.

## 2.6 Ferrocene aerogel synthesis

Iron-doped organic aerogels were synthesized according to the data presented in the studies of Bolobajev et al. (2019) and Kask (2017).

The precursors used for the synthesis of ferrocene aerogels were 5-methylresorcinol and ferrocenylmethanol. Both compounds participate in polymerization reaction with formaldehyde forming an organic gel (Sol-Gel process). Sol-Gel process results in aggregation of colloidal particles with the following formation of three-dimensional interconnected structure. This is an essential prerequisite for the resultant structural properties including porosity. Organic gels were dried with supercritical CO<sub>2</sub> using supercritical extraction system performed in the Department of Chemistry and Biotechnology at Tallinn University of Technology.

Synthesis of ferrocene aerogels was based on the molar ratios between ferrocenylmethanol and 5-methylresorcinol (Ferrc/5MR) and conducted according to data from Table 3. The studied ferrocene aerogel was synthesized using Ferrc/5MR = 0.2/0.8.

Table 3. Data for ferrocene aerogels synthesis

<b>Ratio</b>	<b>n(Ferrc), mmol</b>	<b>n(5MR), mmol</b>	<b>m(Ferrc), mg</b>	<b>m(5MR), mg</b>	<b>n(HCHO), mmol</b>	<b>V(HCHO 30%), mL</b>
0.00	0	1.533	0	190.1	4.599	0.34
0.05	0.077	1.456	15.9	180.6	4.522	0.34
0.10	0.153	1.380	31.9	171.1	4.446	0.33
0.15	0.230	1.303	47.8	161.6	4.369	0.32
0.20	0.307	1.226	63.8	152.1	4.292	0.32
0.25	0.383	1.150	79.7	142.6	4.216	0.31
0.30	0.460	1.073	95.7	133.1	4.139	0.31
0.35	0.537	0.996	111.6	123.6	4.062	0.30
0.40	0.613	0.920	127.5	114.1	3.986	0.30
0.45	0.690	0.843	143.5	104.6	3.909	0.29
0.50	0.767	0.767	159.4	95.0	3.833	0.29
0.55	0.843	0.690	175.4	85.5	3.756	0.28
0.60	0.920	0.613	191.3	76.0	3.679	0.27
0.65	0.996	0.537	207.3	66.5	3.603	0.27
0.70	1.073	0.460	223.2	57.0	3.526	0.26
0.75	1.150	0.383	239.1	47.5	3.449	0.26
0.80	1.226	0.307	255.1	38.0	3.373	0.25

The synthesis underwent in the solvent dioxane (4 ml) using 1M hydrochloric acid (315  $\mu$ l) as catalyst. The maximum molar fraction of ferrocenylmethanol could be 0.5. The further increase of the ferrocenylmethanol results in turning the gel to be very fragile and to break down upon extraction. So, the optimum ratio for aerogel synthesis is about 0.2. Molar fractions of formaldehyde was calculated using Equation 16:

$$\frac{n(5\text{-methylresorcinol}) + n(\text{ferrocenylmethanol})}{n(\text{formaldehyde}) + n(\text{ferrocenylmethanol})} = 1:3 \quad (16)$$

The required amounts of resorcinol and ferrocenylmethanol were placed in an 8 ml vial, 4 ml of freshly distilled dioxane and 315  $\mu$ l of 1M hydrochloric acid solution were added. The vial was flushed with nitrogen and placed in a thermostat (Julabo, Germany) at  $t = 60$  °C. The reaction mixture was stirred for 15 min, then cooled down to the room temperature ( $22 \pm 2$  °C) and the required amount of 37% formaldehyde solution was added. The vial was flushed with nitrogen again, placed backed in a water bath, and stirred for an additional 5 minutes. The solution was poured into containers for gelation, purged with nitrogen and kept at 60 °C for 3 days until the formation of a gel was completed (Figure 11a). Afterwards, the gels were removed and immersed in acetone for a week to remove the residual dioxane (Figure 11b). The resultant gels were sent to drying with supercritical CO<sub>2</sub>.

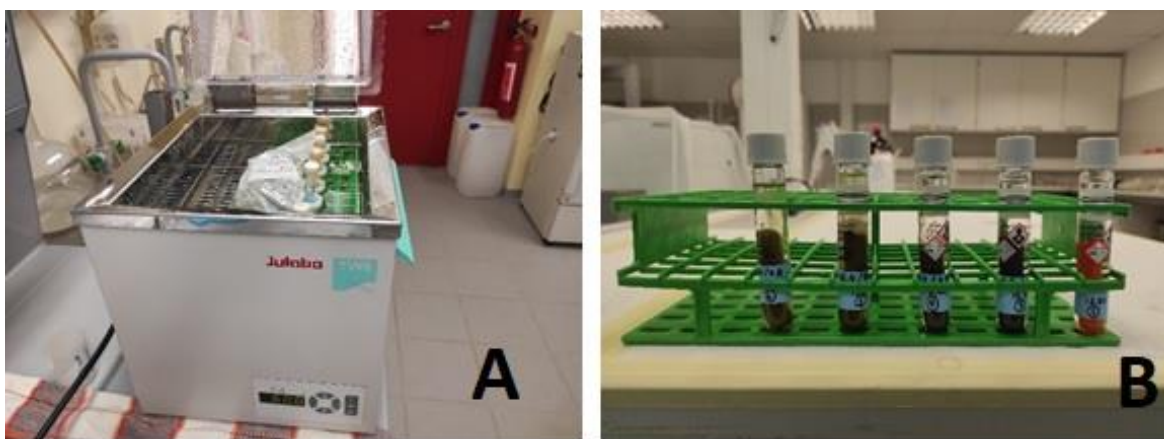


Figure 11. a) Sol-gel process in thermostat; b) resultant ferrocene-gels immersed in acetone

For drying of gels to obtain aerogels were used critical-point drying method in the autoclave in the laboratory of TalTech Chemistry and biology institute.

## 3 RESULTS AND DISCUSSION

### 3.1 Photo-induced degradation of NDEA

In experiments with N-Nitrosodiethylamine the best result was obtained using UV-A photolysis (Figure 12). UV-A lamp, which emits light at wavelength of 315–400 nm, was chosen because previous experiments in degradation NDEA with UV-C lamp showed excellent result in 4 minutes (Jaaksaar, 2020), so there was no need to conduct these tests again. Also, the application of UV-A lamp for photo-induced degradation of NDEA was aimed to obtain slower degradation rate making the comparison with experiments on ferrocene-aerogels technically feasible.

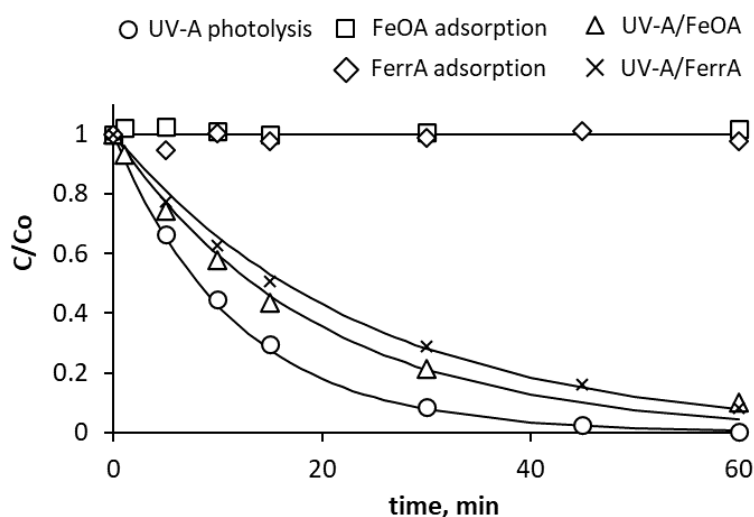


Figure 12. Comparison of photolytic and photo-induced degradation of N-nitrosodiethylamine FeOA stands for iron-doped organic aerogel, FeA for ferrocene aerogel

Degradation of contaminant during photolytic processes occurs by absorption of UV irradiation, which initiates pollutant degradation through direct or indirect photolysis. Direct photolysis is proceeded through absorption of UV irradiation by organic compounds, which induces their reaction with water constituents or causes self-decomposition. Absorption of UV irradiation by water molecules produces oxygen, hydroxyl and peroxide radicals, which react with organic compounds during indirect photolysis. (Chirwa & Bamuzza-Pemu, 2010) According to process description, it fits into pseudo-first order reaction kinetics. A simplified pseudo-first order reaction kinetics equation (Equation 17) is used for the practical evaluation of the photolytic and photo-induced process control mechanism for degradation of N-nitrosodiethylamine, accepting the flux of photons emitted by the light source to be uniform, the temperature and

volume of the solution to be constant, and mixing of the solution in the reactor to be ideal:

$$\ln \frac{C_0}{C} = kt \quad (17)$$

$C_0$  - initial concentration (M)

$C$  - obtained concentration (M)

$k$  - the reaction rate constant

$t$  - time (min) (Wang et al., 2021).

Reaction rate constants presented in Table 4 for photo-induced degradation of NDEA were obtained by fitting kinetics data into Equation 17 with subsequent linear regression analysis.

Table 4. Reaction rate constants for applied photo-induced degradation methods of N-nitrosodiethylamine  
 UV-A/FerrA stands for photo-induced degradation with ferrocene aerogel  
 UV-A/FeOA stands for photo-induced degradation with iron-doped organic aerogel  
 R is the correlation coefficient for linear regression

<b>Method</b>	<b>k (min<sup>-1</sup>)</b>	<b>R<sup>2</sup></b>
UV-A photolysis	0.0858	0.9881
UV-A/FerrA	0.0419	0.9988
UV-A/FeOA	0.0386	0.9697

The complete degradation of N-nitrosodiethylamine by UV-A photolysis was achieved within 45 min, whereas the identical experiments performed by Jaaksaar (2020) resulted in 60% of NDEA degradation after 60 min. Jaaksaar (2020) had also calculated reaction rate constant for NDEA degradation by UV-A photolysis, which was obtained to be  $k = 0.0168 \text{ (min}^{-1}\text{)}$  with the correlation coefficient for linear regression  $R^2 = 0.9937$ . As it is seen from results, UV-A photolysis during experiments in present study was more rapid and intense. Such disparity could be explained by different geometry of the reactors used in both studies. Construction features of the present reactor allowed achieving better result. In general, the efficacy of photolysis method for degradation of N-nitrosodiethylamine indicates that NDEA is light-sensitive possessing NDEA quantum yield  $\Phi = 0.392 \text{ M/Einstein}$  in UV-A light region. Results of other studies confirm that NDEA is very sensitive towards ultraviolet radiation (Plumlee & Reinhard, 2007; Jaaksaar, 2020).

Adsorption test with ferrocene aerogels and iron-doped organic aerogels showed no significant concentration decrease in aqueous phase, which means that studies aerogels did not tend to adsorb NDEA. It is known that powdered activated carbon commonly used for adsorption process in water treatment is able to adsorb 89.4% of N-nitrosodiethylamine and 80.5% of N-nitrosodimethylamine from aqueous solutions (Aygün, Uyanık & Batı, 2004).

UV-A photo-induced degradation of NDEA in the presence of either ferrocene aerogel, or iron-doped organic aerogel did not show some remarkable effect on degradation rate of studied pollutant. By comparing these experiments with UV-A photolysis it is obvious that the degradation rate is slightly higher in the absence than in the presence of aerogels. This indicates that degradation of NDEA occurred under the influence of UV-A light only and studied aerogels did not induce the degradation. Moreover, suspended aerogels particles caused the obstruction for the penetration of UV-A light reducing slightly the rate of NDEA photolysis. According to the data obtained the application of aerogels in photo-induced degradation of N-nitrosodiethylamine could not be considered as an expedient method, so the hypothesis H1 is not confirmed for NDEA.

### **3.2 Photo-induced degradation of TMP**

For photo-induced degradation of trimethoprim both UV-A (emitted light wavelength is 315–400 nm) and UV-C lamps (emitted light wavelength is 200–280 nm) were applied (Figure 13). Experiments with iron-doped organic aerogels for adsorption of trimethoprim were conducted in previous studies (Bolobajev et al., 2019; Bolobajev, Kask & Koel, 2019; Kask, 2017), so there was no need to conduct this experiments again.

Same as for N-nitrosodiethylamine, reaction rate constants for photo-induced degradation of TMP were obtained by fitting kinetics data into Equation 17 with subsequent linear regression analysis (Table 5).

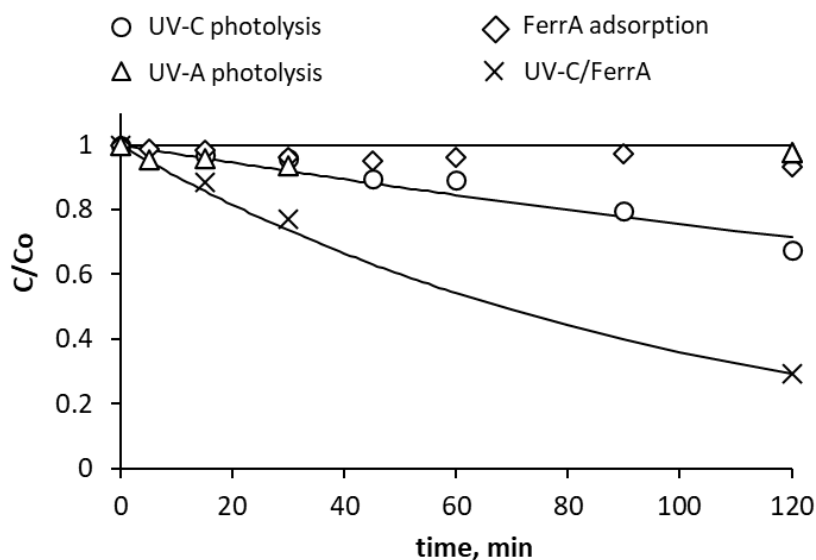


Figure 13. Photoinduced degradation of trimethoprim  
 FeOA stands for iron-doped organic aerogel, FeA for ferrocene aerogel

Table 5. Reaction rate constants for applied photo-induced degradation methods of trimethoprim  
 UV-C/FerrA stands for photo-induced degradation with ferrocene aerogel  
 R is the correlation coefficient for linear regression

Method	k (min <sup>-1</sup> )	R <sup>2</sup>
UV-A photolysis	0.0022	0.9809
UV-C photolysis	0.0023	0.9581
UV-C/FerrA	0.0105	0.9983

UV-A photolysis showed no significant result in degradation of trimethoprim. This is similar to the result obtained in another research, where aqueous solution with the same initial concentration of TMP ( $C_0 = 10 \mu\text{M}$ ) were irradiated with UV-A light (Bolobajev, Kask & Koel, 2019). The TMP light absorption spectrum (Figure 14) shows that no absorption occurs at wavelengths  $> 315 \text{ nm}$ . So result of UV-A photolysis obtained in current study correlates with light adsorption spectrum of trimethoprim.

Application of the UV-C lamp for photolysis resulted in better degradation of trimethoprim with more than 30% reduction of initial concentration within 120 min. This is similar to the result of another study, where under UV-C irradiation half of the same initial concentration of TMP ( $C_0 = 10 \mu\text{M}$ ) were degraded within 120 min (Bolobajev, Kask & Koel, 2019).

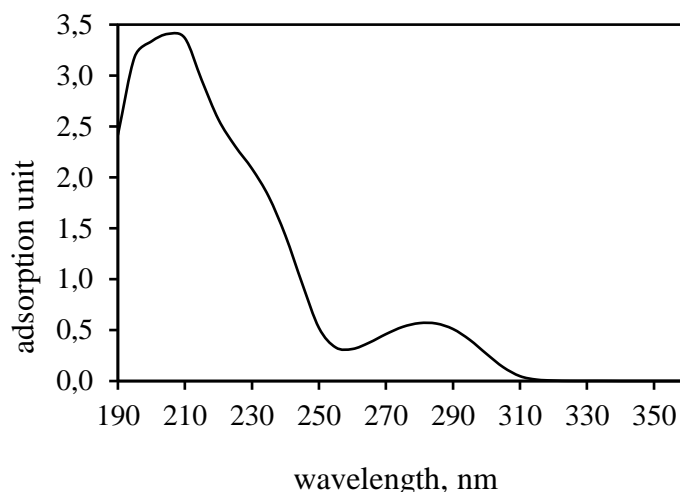


Figure 14. Light absorption spectrum of trimethoprim at neutral pH (Kask, 2017)

Obtained result also correlates with light adsorption spectrum of TMP (Figure 14), which is the most intense around wavelength of 210 nm. From photolysis experiments can be concluded that trimethoprim is absolutely not sensitive to UV-A irradiation and little sensitive to UV-C irradiation. Obtained results testify that trimethoprim is not light-sensitive compound, which is also proved by TMP quantum yield  $\Phi = 0.0017$  M/Einstein.

Adsorption test with ferrocene aerogels showed no significant result. Trimethoprim is a weak base with value of the acid dissociation constant (pKa) of 7.2 and could be adsorbed to negatively charged surfaces by cation-exchange process, whereas the physical adsorption could take place due to hydrophobic interactions (Van der Waals forces) (Perez et al., 2020). Bolobajev, Kask & Koel (2019) conducted similar study on metal-doped aerogels and found out that the efficacy of aerogels adsorption depends on surface area and porosity. For example, nickel-doped organic aerogel adsorbed 40% of initial TMP concentration within 120 min. (Bolobajev, Kask & Koel, 2019). The weak adsorption ability of the ferrocene aerogels needs the following research.

Insofar as UV-C photolysis showed better result than UV-A photolysis and UV-C light spectrum is better absorbed by trimethoprim, UV-C lamp was chosen for photo-induced degradation with the ferrocene aerogel. It is clear that in the presence of ferrocene aerogels the degradation of TMP under UV-C light was significantly faster than that of mere UV-C photolysis, which might indicate the photo-induced processes, or even photocatalysis. So the hypothesis H1 is confirmed for trimethoprim. In another study, metal-doped aerogels were successfully applied in heterogeneous photocatalysis for degradation of trimethoprim (Bolobajev, Kask & Koel, 2019). Applying nickel-doped organic aerogels resulted in four-fold reduction in TMP concentration in comparison to

photolysis (Bolobajev, Kask & Koel, 2019). Photocatalytic ability of metal containing aerogels was described by Jiang et al. (2021) as well. However, the assumption of the presence of photocatalysis needs the following research.

### 3.3 Actinometry and quantum yield

Quantum yield determines the susceptibility of a contaminant to photolytic degradation (Braslavsky, 2007). The quantum yields of N-nitrosodiethylamine and trimethoprim were calculated using the UV-A and UV-C light intensity determined in the actinometry experiments (Figure 15), which was compared with the results of photolytic degradation experiments. The intensity of light (Table 6) was found using Equation 17 (Braslavsky, 2007).

$$I = \frac{N}{\Phi_{Fe}t(1-10^{\epsilon l[A]})} \approx \frac{N}{\Phi_{Fe}t} \quad (17)$$

$\Phi_{Fe}$  - the quantum yield of ferrioxalate (1.25 mol/Einstein)  
 $N$  - the number of moles (moles) of Fe (II) formed  
 $(1-10^{\epsilon l[A]})$  - the light absorbed by the actinometric solution (usually taken as 1)  
 $t$  - time (min)

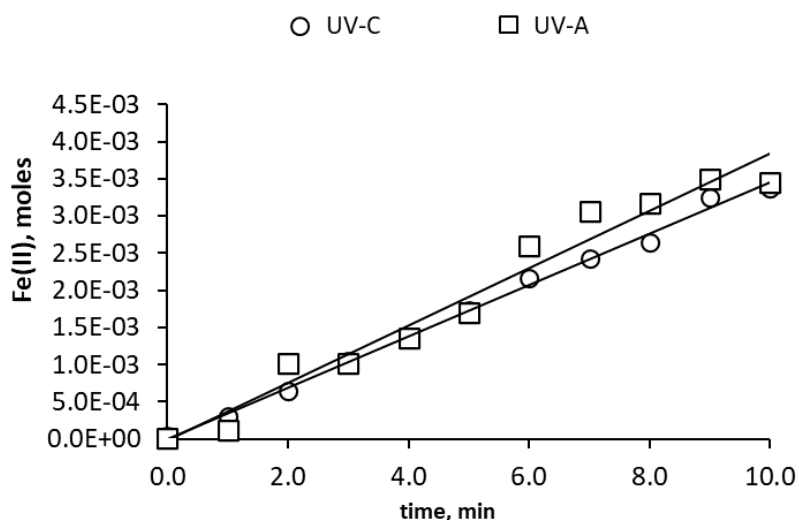


Figure 15. Fe(II) moles formed from ferrioxalate under the irradiation with UV-A and UV-C light

Radiation intensity calculations for UV-C and UV-A lamps are presented in Table 6, calculations in photons per minute were performed according to the Equation 18 (Braslavsky, 2007):

$$I \approx \frac{N \cdot N_A}{\Phi_{Fe} t} \quad (18)$$

$N_A$  - Avogadro constant ( $6.022 \cdot 10^{23} \text{ mol}^{-1}$ )

Table 6. Results of actinometry for UV-A and UV-C lamps

	<b>UV-C</b>	<b>UV-A</b>
Radiation intensity in reactor I, Einstein/min	$2.72 \cdot 10^{-6}$	$2.91 \cdot 10^{-6}$
Radiation intensity in reactor, hv/min	$1.64 \cdot 10^{18}$	$1.75 \cdot 10^{18}$

The quantum yield of contaminants (Table 7) was calculated by Equation 19 (Braslavsky, 2007):

$$\Phi = \frac{\Delta N_t}{I t} \quad (19)$$

$\Delta N_t$  - the concentration decrease caused by photolysis per unit of time

Table 7. Quantum yields of NDEA under UV-A irradiation and TMP under UV-C irradiation

	<b>Trimethoprim (UV-C)</b>	<b>N-nitrosodiethylamine (UV-A)</b>
Quantum yield, M/Einstein	0.0017	0.392

Obtained quantum yield results show that NDEA is more sensitive towards photolytic degradation than trimethoprim, which is also obvious from photolytic experiments. In another study, the quantum yield of trimethoprim under UV-C irradiation was equal to 0.0019 M/Einstein (Bolobajev et al., 2019), which is similar to result obtained in the present study. The quantum yield for antibiotic sulfamethoxazole (SMX), which is used in combination with trimethoprim (WHO, 2019), is found to be  $0.046 \pm 0.021$  M/Einstein (Canonica, Meunier & von Gunten, 2008). This means that sulfamethoxazole is more sensitive to photodegradation than trimethoprim, so further investigation of photo-

induced degradation with ferrocene aerogels could include SMX or the combination of both antibiotics.

The quantum yield of NDEA under simulated sun-light irradiation was determined as 0.43 M/Einstein (Plumlee & Reinhard, 2007). This is close to the result obtained in current study despite the differences in experimental conditions. For N-nitrosodimethylamine (NDMA), which is another byproduct of chloramination (Kodamatani et al., 2021), the quantum yield was found to be 0.3 M/Einstein (Sharpless & Linden, 2003). In another study, it was obtained to be 0.41 M/Einstein (Plumlee & Reinhard, 2007). Quantum yields for other nitrosoamines, such as N-nitrosopiperidine (NPip), N-nitrosomethylethylamine (NMEA), N-nitrosodipropylamine (NDPA), N-nitrosodibutylamine (NDBA) and N-nitrosopyrrolidine (NPYR) lie in the range between 0.43–0.61 M/Einstein (Plumlee & Reinhard, 2007). This means that nitrosoamines are very sensitive to photolytic degradation, so photolysis should be an appropriate method for post-chloraminated water treatment in order to degrade this byproducts.

## **3.4 Fenton experiments**

### **3.4.1 Experiments with NDEA**

FerrA and FeOA contain iron within the structure, which could possible promote the Fenton-like oxidation. The occurrence of Fenton-mediated oxidation was curious from scientific standpoint, so the degradation of NDEA was tested using the classical Fenton reagent and ferrocene and iron-doped organic aerogels as a possible Fenton-like catalysts (Figure 16). Constants were not calculated due to multi-step character of Fenton reaction.

Fenton reagent showed moderate ability to degrade NDEA with flattening curve at concentration of 8  $\mu\text{M}$ , which is about 70% of initial concentration. Possibly, the limit for Fenton reagent's ability to degrade NDEA was reached at this concentration.

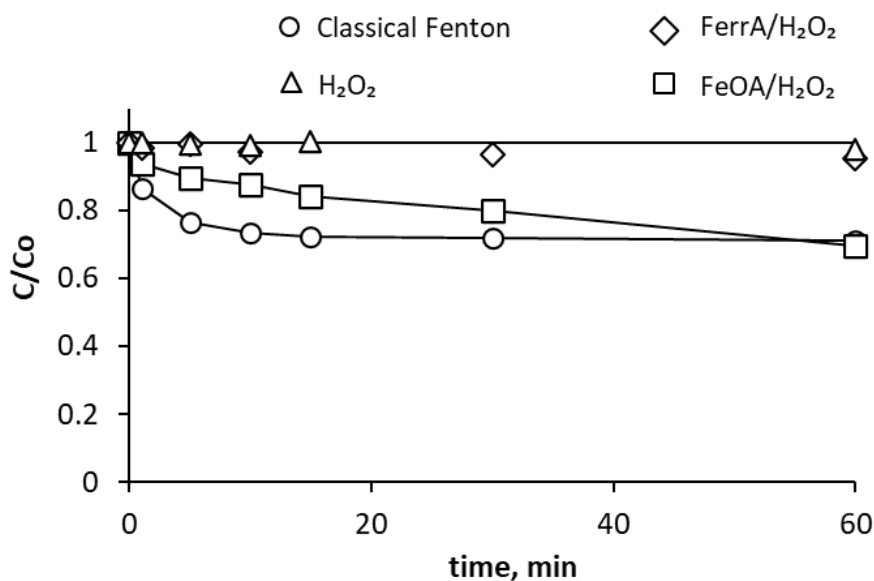


Figure 16. Results of Fenton and Fenton-like reactions experiments with NDEA FeOA stands for iron-doped organic aerogel, FerrA for ferrocene aerogel

According to Pignatello, Oliveros & MacKay (2006), oxidation of contaminants in Fenton reaction occurs by generation of hydroxyl radicals HO• (Equation 18). Fe(II) is oxidized quickly (1-2 min) to Fe(III) and generation of HO• slows down. Fe(III) could be reduced according to reaction (Equation 19), which plays the role of rate-limiting step, as it is considerably slower than Equation 18.



So Fe(III) is accumulating and complexating with carboxylate species produced from degraded organic matter, which reduces the degradation rates of the Fenton reaction. Fenton reaction is rapid at the first minutes, but with the oxidation of iron reaction is fading. (Pignatello, Oliveros & MacKay, 2006)

Ferrocene aerogel did not succeed in degrading NDEA in Fenton-like reaction. Iron-doped organic aerogel's ability to degrade NDEA in Fenton-like reaction was comparable to Fenton reagent. It should be mentioned that degradation with Fenton-like reaction using iron-doped organic aerogels was slower than with Fenton reagent. On the other hand, differently from Fenton reagent, iron-doped organic aerogel's curve is not flatter and continues to fall, which means that Fenton-like reaction has not stopped. In comparative study of degrading dye with Fenton and Fenton-like reagents similar result was achieved: degradation with Fenton-like reagent was slower, but achieved the

same result as Fenton reagent within 100 min (Wang S. 2008). This may indicate the potential of iron-doped organic aerogels to degrade NDEA in Fenton-like reaction at slow rate and low concentrations. Iron-doped organic aerogels are possibly Fenton-like reagent, so the hypothesis H2 is partially confirmed in experiments with NDEA. However, this method is not so effective comparing to photolysis, hence it is not preferable one for degradation of NDEA.

### 3.4.2 Experiments with TMP

Same as for N-nitrosodiethylamine, classic Fenton reaction and Fenton-like reactions with ferrocene and iron-doped organic aerogels were applied for degradation of trimethoprim (Figure 17). Constants were not calculated due to multi-step character of Fenton reaction.

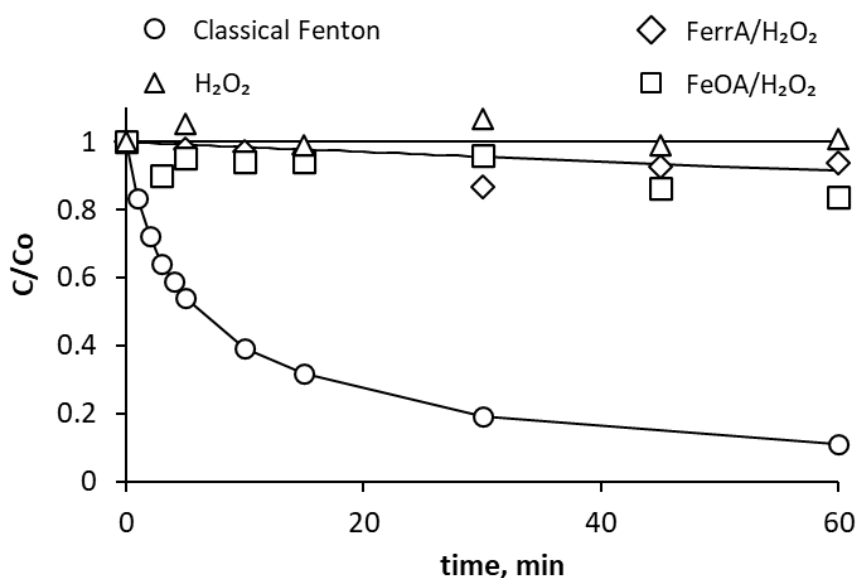


Figure 17. Results of Fenton and Fenton-like degradation of TMP  
 FerrA/H<sub>2</sub>O<sub>2</sub> stands for Fenton-like degradation with ferrocene aerogel  
 FeOA/H<sub>2</sub>O<sub>2</sub> stands for Fenton-like degradation with iron-doped organic aerogel

Classic Fenton reaction showed great result in degrading trimethoprim. This result corresponds with results achieved in another field study (Wang & Wang, 2017), where TMP was successfully degraded using Fenton process. However, there are certain disadvantages for classic Fenton process application in water treatment. Suitable pH range for Fenton process is around 3 (Pignatello, Oliveros & MacKay, 2006). So pH of treated water should be adjusted prior to using this method. In classic Fenton process iron containing sludge is produced (Zhu et al., 2021). Threshold for iron in drinking

water is established to be 200 µg/l in European Union by Council Directive 98/83/EC (Council of the European Union, 1998). So, filtration step is needed to eliminate iron from water. Furthermore, active components such as hydrogen peroxide should be separated from the reaction solution (Zhu et al., 2021). So, additional purification steps that should be applied after Fenton process raise the cost of the treatment. All discussed disadvantages are making application of classic Fenton process costly and complicated.

Same as for NDEA, applying iron-doped organic aerogel showed some ability to degrade trimethoprim in Fenton-like process. So, iron in the structure of iron-doped organic aerogels was participating in both reactions with NDEA and TMP. According to obtained results iron-doped organic aerogels can serve as Fenton-like reagents, which partially confirm the hypothesis H2, so further investigation can be done in this field. As degradation rate of TMP with iron-doped organic aerogel as Fenton-like reagent was slow, hence this method is not preferable for degradation of trimethoprim.

Applying ferrocene aerogels for Fenton-like reaction showed no significant result in degradation of trimethoprim. So, the hypothesis H2 about possibly occurring Fenton-like process with ferrocene aerogels was not confirmed. This result gives another evidence in favor of the hypothesis H1 about occurring photo-induced reaction in presence of ferrocene aerogels in water solution of trimethoprim. Thus it can be concluded that degradation of trimethoprim under UV-C light was photo-induced in presence of ferrocene aerogels, so hypothesis H1 is partially confirmed for ferrocene aerogels and TMP. According to this finding ferrocene aerogels can be suggested as catalysts for degradation of trimethoprim in presence of UV-C light.

As a suggestion for further implication of ferrocene aerogels in water treatment, fluidized bed reactor with an UV-C lamp can be a good choice, because it allows to easily collect catalyst after reaction. Also, in comparison to packed bed reactors, fluidized bed reactors require less catalyst loading. As a result, the pressure drop during water pumping through the reactor is lower and the exposure of photocatalysts to light is improved. Due to set up of this system, catalysts are suspended by the upward flow of water. So, catalysts float in the stream. (Matoh et al., 2019)

Furthermore, mentioned reactor type was successfully implied in photocatalytic degradation processes with aerogels. In field study (Rincón & La Motta, 2019) fluidized bed photocatalytic reactor with UV-C lamp were applied to degrade phenol using TiO<sub>2</sub> covered silica gel. Silica gel was used as a bed and TiO<sub>2</sub> as catalyst, synthesized by sol-gel process. Results show that efficiency of this configuration for photocatalysis is only

30% less than that of suspended TiO<sub>2</sub>. On the other hand, this method eliminates the need for additional steps for separation and catalyst recovery from the effluent solution, which tend to be major drawbacks for application of photocatalysis on large scale. In addition, this method maximizes photon-exposed area of catalyst and allows to conduct continuous operation. (Rincón & La Motta 2019)

So this method can be more sustainable and cost effective for treatment of trimethoprim than classic Fenton process due to absence of secondary pollution, which eliminates the need for additional filtration and another after-treatment steps. It is important to further study this field in order to develop the best suitable technology for implication of ferrocene aerogels in water treatment.

## SUMMARY

The present study was intended to examine the ability of ferrocene and Fe-doped aerogels to induce photo-degradation of micropollutants trimethoprim (TMP) and N-nitrosodiethylamine (NDEA). For that purpose, series of treatment methods were studied in the presence and in the absence of aerogels. Treatment methods included photolysis, photo-induced process with aerogels, classical Fenton and Fenton-like treatment with aerogels. Reaction kinetics and quantum yield of examined contaminants were calculated. NDEA was found to be light-sensitive, which is consistent with the results of photolysis experiments studied previously. Ferrocene aerogel was synthesized in the Laboratory of Environmental Technology for the first time. Its application in environmental technology has been studied. Thesis was intended to widen applications of studied aerogels in water treatment. This aim is completed to some point, but further study is needed in this field.

According to the data obtained in this study the following conclusions could be made:

- Neither ferrocene nor iron-doped organic aerogels showed remarkable result in photo-assisted degradation of NDEA, because NDEA was found to be photosensitive, and it was easily degraded by photolysis in UV-A and UV-C light region.
- With respect to experiments on degradation of trimethoprim, ferrocene aerogel induced clearly the photo-degradation of this antibiotic. Further research should be done to determine process characteristics and the effective ratio of aerogels precursors, i.e. ferrocenyl methanol and 5-methylresorcinol, for the Sol-Gel synthesis of most appropriate ferrocene aerogel. In addition, further research should be focused on the testing of photocatalytic properties of studied materials.
- Another possible suggestion is to test antibiotic sulfamethoxazole, which is commonly used in combination with TMP, for photo-induced degradation with ferrocene aerogels. In addition, suggestion for implication of ferrocene aerogels in water treatment processes is fluidized bed reactor, but optimal operation conditions should be examined in further researches.
- To study the possible Fenton-based reactions occurring by application of ferrocene and Fe-doped aerogels, the corresponding experiments were conducted in the present research. As a result, ferrocene aerogel did not show remarkable activity in the Fenton-like oxidation of studied micropollutants, whereas iron-doped organic aerogel showed ability to perform Fenton-like reaction. The lack of Fenton processes in case of ferrocene aerogel could possibly indicate the photocatalytic properties. However, in terms of materials science a

thorough research of ferrocene aerogels should be done prior to confirmation of photocatalytic properties.

In conclusion, aerogels as materials deserve further research for their future application in water treatment technologies.

## KOKKUVÕTE

Käesoleva töö eesmärk oli uurida ferrotseeni ja rauagalegeeritud aerogeelide mõju mikrosaaainete trimetoprim (TMP) ja N-nitrosodietüülamiin (NDEA) lagundamise erinevates töötlemise protsessides. Uuriti mitmeid töötlusmeetodeid koos aerogeelidega ja ilma. Töötlusmeetoditeks olid fotolüüs, foto-indutseeritud protsess aerogeelidega, klassikaline Fenton ja Fentoni-sarnane töötlemine. Üldiseks sihiks oli laiendada magistritöös kasutatud aerogeelide rakendamist veetöötlustes. Ferrotseeni aerogeel sünteesiti keskkonnatehnoloogia laboris. Töö raames uuriti saasteainete reaktsioonikineetikat ja arvutati kvantsaagis.

Uuringus saadud andmete põhjal võib teha järgmised järeldused:

- Leiti, et NDEA on valgustundlik ja laguneb kergesti UV-A ja UV-C valguse toimel ilma märkimisväärse mõjuta ferrotseeni sisaldavate aerogeelide või rauaga legeeritud orgaaniliste aerogeelide juuresolekul.
- Leiti, et TMP fotolagundamise tõhusus tõusis märgatavalt ferrotseeni aerogeeli juuresolekul, mis viitab fotokatalüütilistele omadustele.
- Enne ferrotseeni aerogeelide fotokatalüütiliste omaduste kinnitamist tuleks antud materjali veelgi põhjalikult uurida. Sobivaima ferrotseeni aerogeeli Sol-Gel sünteesiks tuleks teha täiendavaid uuringuid, nt määrata aerogeelide lähteainete, ferrotsenüülmetanooli ja 5-metüülresortsinooli optimaalne suhe.
- Edasine uuring antud materjalide fotokatalüütiliste omaduste testimise eesmärgil võiks olla antibiootikumi sulfametoksasool, mida tavaliselt kasutatakse koos TMP-ga, lagundamine. Lisaks võiksid ferrotseeni aerogeelid leida rakendust veepuhastusprotsessides keevkihtreaktorites, ent see vajab samuti edasisi uuringuid optimaalsete töötingimuste leidmiseks.
- Uurimaks võimalikke Fenton reaktsioone, mis võivad kulgeda ferrotseeni või rauda sisaldavate aerogeelide kasutamisel, viidi käesolevas uuringus läbi vastavad katsed. Ferrotseeni aerogeel ei näidanud uuritavate mikrosaaainete fentonilaadses oksüdatsioonis märkimisväärset aktiivsust, samas kui Fenton protsess ilmnas rauaga legeeritud orgaanilise aerogeeli juuresolekul.

Kokkuvõtvalt võib öelda, et aerogeelid kui materjalid väärivad täiendavat uurimist nende edaspidiseks rakendamiseks veepuhastustehnoloogiates.

## LIST OF REFERENCES

Alemán, J. V., Chadwick, A. V., He, J., Hess, M., Horie, K., Jones, R. G., Kratochvíl, P., Meisel, I., Mita, I., Moad, G., Penczek, S., & Stepto, R. F. T. (2007). Definitions of terms relating to the structure and processing of sols, gels, networks, and inorganic-organic hybrid materials. *IUPAC Recommendations 2007*, 1806. DOI: <https://doi.org/10.1351/pac200779101801>

Alwin, S., & Shajan, S. X. (2020). Aerogels: promising nanostructured materials for energy conversion and storage applications. *Mater Renew Sustain Energy*, 9, 7. DOI: <https://doi.org/10.1007/s40243-020-00168-4>

Arti, S., Kaur, K., Kaur, J., Ghosh, T. K., Banipal, T. S., & Banipal, P. K. (2021). Host-guest interaction of trimethoprim drug with cyclodextrins in aqueous solutions: calorimetric, spectroscopic, volumetric and theoretical approach. *Journal of Molecular Liquids*, 329, 115431. DOI: <https://doi.org/10.1016/j.molliq.2021.115431>

Aygün, S., Uyanık, A., & Batı, B. (2004). Adsorption of N-nitrosodiethylamine and N-nitrosodimethylamine on activated carbon: a pre-concentration procedure for gas chromatographic analysis. *Microchim. Acta*, 146, 279–283. DOI: <https://doi.org/10.1007/s00604-004-0225-3>

Barb, W. G., Baxendale, J. H., George, P., & Hargrave, K. R. (1951). Reactions of ferrous and ferric ions with hydrogen peroxide. *Transaction of the Faraday Society*, 47, 591–616. DOI: <https://doi.org/10.1039/TF9514700462>

Beltrán, F. J., Rivas, F. J., & Montero-de-Espinosa, R. (2002). Catalytic ozonation of oxalic acid in an aqueous TiO<sub>2</sub> slurry reactor. *Applied Catalysis Part B: Environmental*, 39(3), 221-231. DOI: [https://doi.org/10.1016/S0926-3373\(02\)00102-9](https://doi.org/10.1016/S0926-3373(02)00102-9)

Bheekhun, N., Talib, A. R. A., & Hassan, M. R. (2013). Aerogels in aerospace: an overview. *Advances in Materials Science and Engineering*, 2013, 406065. DOI: <https://doi.org/10.1155/2013/406065>

Bigall, N. C., Herrmann, A.-K., Vogel, M., Rose, M., & Simon, P., Carrillo-Cabrera, W., Dorfs, D., Kaskel, S., Gaponik, N., Eychmüller, A. (2009). Hydrogels and aerogels from noble metal nanoparticles. *Angewandte Chemie International Edition*, 48, 9731-9734. DOI: <https://doi.org/10.1002/anie.200902543>

Bolobajev, J., Kask, M., & Koel, M. (2019) Application of metal-doped organic aerogels for photodegradation of antibiotics in water. *Chemical Industry Digest, June 2019* 92-95.

Bolobajev, J., Kask, M., Kreek, K., Kulp, M., Koel, M., & Goi, A. (2019) Metal-doped organic aerogels for photocatalytic degradation of trimethoprim. *Chemical Engineering Journal, 357*, 120-128. DOI: <https://doi.org/10.1016/j.cej.2018.09.127>

Bond, T., Templeton, M. R., & Graham, N. (2012). Precursors of nitrogenous disinfection by-products in drinking water--A critical review and analysis. *Journal of Hazardous Materials, 235-236*, 1-16. DOI: <https://doi.org/10.1016/j.jhazmat.2012.07.017>

Borsagli, F. G. L. M., & Paiva, A. E. (2021). Eco-friendly luminescent ZnO nanoconjugates with thiol group for potential environmental photocatalytic activity. *Journal of Environmental Chemical Engineering, 9(4)*, 105491. DOI: <https://doi.org/10.1016/j.jece.2021.105491>

Braslavsky, S. E. (2007). Glossary of terms used in photochemistry 3rd edition (IUPAC recommendations 2006). *Pure Appl. Chem., 79(3)*, 293-465. DOI: [doi:10.1351/pac200779030293](https://doi.org/10.1016/j.pac.2007.07.029)

Brooke, J. S. (2014). New strategies against *Stenotrophomonas maltophilia*: a serious worldwide intrinsically drug-resistant opportunistic pathogen. *Expert Review of Anti-infective Therapy, 12(1)*, 1-4. DOI: <https://doi.org/10.1586/14787210.2014.864553>

Buchanan, W., Roddick, F., & Porter, N. (2006). Formation of hazardous by-products resulting from the irradiation of natural organic matter: comparison between UV and VUV irradiation. *Chemosphere, 63*, 1130-1141. DOI: <https://doi.org/10.1016/j.chemosphere.2005.09.040>

Burpo, F., Nagelli, E., Morris, L., McClure, J., Ryu, M., & Palmer, J. (2017). Direct solution-based reduction synthesis of Au, Pd, and Pt aerogels. *Journal of Materials Research, 32(22)*, 4153-4165. DOI: <https://doi.org/10.1557/jmr.2017.412>

Canonica, S., Meunier, L., & von Gunten, U. (2008). Phototransformation of selected pharmaceuticals during UV treatment of drinking water. *Water Research, 42 (1-2)*, 121-128. DOI: <https://doi.org/10.1016/j.watres.2007.07.026>

Chandrasekaran, N., & Adarsh, K.S. (2021). Chapter 7 - Pristine, transition metal and heteroatom-doped carbon aerogels for catalytic and electrocatalytic applications. In Sadjadi S. (Ed.). *Emerging Carbon Materials for Catalysis (235-253)*, Amsterdam: Elsevier. DOI: <https://doi.org/10.1016/B978-0-12-817561-3.00007-X>

Chen, K., Xu, W., Du, A., Shen, J., Wu, G., Bao, Z., & Zhou, B. (2014). Template confined synthetic strategy for three-dimensional free-standing hierarchical porous nanocrystalline tantalum. *Materials Letters*, *116*, 31-34. DOI: <https://doi.org/10.1016/j.matlet.2013.10.079>

Chen, W.-H., Wang, Y.-H., & Hsu, T. H. (2021). The competitive effect of different chlorination disinfection methods and additional inorganic nitrogen on nitrosamine formation from aromatic and heterocyclic amine-containing pharmaceuticals. *Chemosphere*, *267*, 128922. DOI: <https://doi.org/10.1016/j.chemosphere.2020.128922>

Chen, Y., Chen, W., Huang, H., Zeng, H., Tan, L., Pang, Y., Ghani, J., & Qi, S. (2021). Occurrence of N-nitrosamines and their precursors in the middle and lower reaches of Yangtze River water. *Environmental Research*, *195*, 110673. DOI: <https://doi.org/10.1016/j.envres.2020.110673>

Chirwa, E., & Bamuza-Pemu, E. (2010). Investigation of photocatalysis as an alternative to other advanced oxidation processes for the treatment of filter backwash water. DOI: <https://doi.org/10.13140/RG.2.1.1368.3042>

Choi, Y., Koo, M.S., Bokare, A.D., Kim, D.H., Bahnemann, D.W., & Choi W. (2017). Sequential process combination of photocatalytic oxidation and dark reduction for the removal of organic pollutants and Cr(VI) using Ag/TiO<sub>2</sub>. *Environ Sci Technol*, *51* 3973-3981. DOI: <https://doi.org/10.1021/acs.est.6b06303>

Condliffe, J. (2014). *Amazing aerogel: eight looks at the ghostly supermaterial in action*. Retrieved from <https://bit.ly/3yE0Fgb>

Council of the European Union (1998). Council Directive 98/83/EC of 3 November 1998 on the quality of water intended for human consumption. *Official Journal L*, *330*, 0032 – 0054. Retrieved from <https://bit.ly/3uktM4O>

Das, S., & Mahalingam, H. (2020). Novel immobilized ternary photocatalytic polymer film based airlift reactor for efficient degradation of complex phthalocyanine dye wastewater. *J Hazard Mater*, *383*, 121219. DOI: <https://doi.org/10.1016/j.jhazmat.2019.121219>

Demas J. N., Bowman W. D., Zalewski E. F., & Veiapoidi R. A. (1981). Determination of the quantum yield of the ferrioxalate actinometer with electrically calibrated radiometers. *The Journal of Physical Chemistry*, *85*, 2766–2771. DOI: <https://doi.org/10.1021/j150619a015>

Deng, F., Shi, H., Guo, Y., Luo, X., & Zhou, J. (2021). Engineering paths of sustainable and green photocatalytic degradation technology for pharmaceuticals and organic contaminants of emerging concern. *Current Opinion in Green and Sustainable Chemistry*, *29*, 100465. DOI: <https://doi.org/10.1016/j.cogsc.2021.100465>

Deng, Y., Liu, J., Huang, Y., Ma, M., Liu, K., Dou, X., & Wang, Z. (2020). Engineering the photocatalytic behaviors of g/C<sub>3</sub>N<sub>4</sub>-based metal-free materials for degradation of a representative antibiotic. *Advanced Functional Materials*, *30*, 2002353. DOI: <https://doi.org/10.1002/adfm.202002353>

Druzian, S. P., Zanatta, N. P., Borchardt, R. K., Côrtes, L. N., Streit, A. F. M., Severo, E. C., Gonçalves, J. O., Foletto, E. L., Lima, E. C., & Dotto, G. L. (2021). Chitin-psyllium based aerogel for the efficient removal of crystal violet from aqueous solutions. *International Journal of Biological Macromolecules*, *179*, 366-376. DOI: <https://doi.org/10.1016/j.ijbiomac.2021.02.179>

Du, R., Wang, J., Wang, Y., Hübner, R., Xuelin, F., Senkovska I., Yue, H., Kaskel S., & Eychmüller, A. (2020). Unveiling reductant chemistry in fabricating noble metal aerogels for superior oxygen evolution and ethanol oxidation. *Nat Commun*, *11*, 1590. DOI: <https://doi.org/10.1038/s41467-020-15391-w>

Du, R., Xinyi, J., Hübner, R., Xuelin, F., Yue, H., & Eychmüller, A. (2019). Engineering self-supported noble metal foams toward electrocatalysis and beyond. *Advanced Energy Materials*, *10*(11), 1901945. DOI: <https://doi.org/10.1002/aenm.201901945>

Eddens, T., Wolfe, R., Nowalk, A., Forno, E., & Campfield, B. (2021). Trimethoprim-sulfamethoxazole use is associated with improved lung function in pediatric asthma.

*Journal of Allergy and Clinical Immunology*, 147(2), AB239. DOI: <https://doi.org/10.1016/j.jaci.2020.12.017>

Eliopoulos, G. M., & Huovinen, P. (2001). Resistance to trimethoprim-sulfamethoxazole. *Clinical Infectious Diseases*, 32(11), 1608–1614. DOI: <https://doi.org/10.1086/320532>

Erkhova, L. V., Presniakov, I. A., Afanasov, M. I., Lemenovskiy, D. A., Yu, H., Wang, L., Danilson, M., & Koel, M. (2020). Ferrocene introduced into 5-methylresorcinol-based organic aerogels. *Polymers*, 12(7), 1582. DOI: <https://doi.org/10.3390/polym12071582>

Espíndola, J. C., Cristóvão, R. O., Mendes, A., Rui, A., Boaventura, R., & Vilar, V. J. P. (2019). Photocatalytic membrane reactor performance towards oxytetracycline removal from synthetic and real matrices: suspended vs immobilized TiO<sub>2</sub>-P25. *Chem Eng J*, 378, 122114. DOI: <https://doi.org/10.1016/j.cej.2019.122114>

Fenton, H. J. H. (1894). Oxidation of tartaric acid in presence of iron. *Journal of the Chemical Society*, 65(65), 899–911. DOI: <https://doi.org/10.1039/CT8946500899>

Fujioka, T., Kodamatani, H., Minh Tran, H. D., Fujioka, A., Hino, K., Yoshikawa, T., Inoue, D., & Ikehata, K. (2021) Degradation of N-nitrosamines and 1,4-dioxane using vacuum ultraviolet irradiation (UV<sub>254+185 nm</sub> or UV<sub>172 nm</sub>). *Chemosphere*, 278, 130326. DOI: <https://doi.org/10.1016/j.chemosphere.2021.130326>

Gao, H.-L., Xu, L., Long, F., Pan, Z., Du, Y.-X., Lu, Y., Ge, J., & Yu, S.-H. (2014). Macroscopic free-standing hierarchical 3D architectures assembled from silver nanowires by ice templating. *Angew. Chem. Int. Ed.*, 53, 4561-4566. DOI: <https://doi.org/10.1002/anie.201400457>

García-González, C. A., Sosnik, A., Kalmár, J., De Marco, I., Erkey, C. Concheiro, A., & Alvarez-Lorenzo, C. (2021). Aerogels in drug delivery: from design to application. *Journal of Controlled Release*, 332, 40-63. DOI: <https://doi.org/10.1016/j.jconrel.2021.02.012>

Gilca, A. F., Teodosiu, C., Fiore, S., & Musteret, C. P. (2020). Emerging disinfection byproducts: A review on their occurrence and control in drinking water treatment processes. *Chemosphere*, 259, 127476. DOI: <https://doi.org/10.1016/j.chemosphere.2020.127476>.

Grier, A. J. & Rivkin, A. S. (2019). Chapter 5 - Comparing sample and remote-sensing data—understanding surface composition. In Grier, A. J., & Rivkin, A. S. (Ed.). *Airless Bodies of the Inner Solar System*, (95-119), Amsterdam: Elsevier. DOI: <https://doi.org/10.1016/B978-0-12-809279-8.00005-6>

Guajardo, S., Figueroa, T., Borges, J., Aguayo, C., & Fernández, K. (2021). Graphene oxide-gelatin aerogels as wound dressings with improved hemostatic properties. *Materials Today Chemistry*, 20, 100418. DOI: <https://doi.org/10.1016/j.mtchem.2020.100418>

He, X., Chen, T., Jiang, T., Wang, C., Luan, Y., Liu, P., & Liu, Z. (2021). Preparation and adsorption properties of magnetic hydrophobic cellulose aerogels based on refined fibers. *Carbohydrate Polymers*, 260, 117790. DOI: <https://doi.org/10.1016/j.carbpol.2021.117790>

Hoffmann, M. R., Martin, S.T., Choi, W., & Bahnemann, D. W. (1995). Environmental applications of semiconductor photocatalysis. *Chemical Reviews*, 95, 69-96. DOI: <https://doi.org/10.1021/cr00033a004>

Huang, C., Cai, B., Zhang, L., Zhang, C., & Pan, H. (2021). Preparation of iron-based metal-organic framework @cellulose aerogel by in situ growth method and its application to dye adsorption. *Journal of Solid State Chemistry*, 297, 122030. DOI: <https://doi.org/10.1016/j.jssc.2021.122030>

Huang, Z., Liu, S., Xu, J., Yin, L., Sun, F., Zhou, N., & Ouyang, G. (2018). Fabrication of 8-aminocaprylic acid doped UIO-66 as sensitive solid-phase microextraction fiber for nitrosamines. *Talanta*, 178, 629-635. DOI: <https://doi.org/10.1016/j.talanta.2017.09.090>

Iervolino, G., Vaiano, V., & Palma, V. (2020). Chapter 10 - Membrane technology for photoelectrochemical hydrogen production. In Basile, A., & Napporn, T. W. (Ed.). *Current Trends and Future Developments on (Bio-) Membranes*, (291-306). Amsterdam: Elsevier. DOI: <https://doi.org/10.1016/B978-0-12-817110-3.00010-2>

Interchemie Werken «DE Adelaar» B.V. (2021). *Intertrim-480 WS sulfadiazine & trimethoprim water-soluble powder*. Retrieved from <https://bit.ly/3fCxxNq>

Jaaksaar, M. (2020). Application of ozonation, photolysis and O<sub>3</sub>/H<sub>2</sub>O<sub>2</sub> for the oxidation of N-nitrosodimethylamine and N-nitrosodiethylamine – a comparative study. Tallinn.

Jiang, X., Du, R., Hübner, R., Hu, Y., & Eychmüller, A. (2021). A Roadmap for 3D Metal Aerogels: Materials Design and Application Attempts. *Matter*, 4(1), 54-94. DOI: <https://doi.org/10.1016/j.matt.2020.10.001>

Kask, M. (2017). Metalli sisaldavate orgaaniliste aerogelide fotokatalüütiline mõju trimetoprimi lagundamisele. Tallinn.

Kistler, S. S. (1931). Coherent expanded aerogels and jellies. *Nature*, 127, 741. DOI: <https://doi.org/10.1038/127741a0>

Kistler, S. S. (1932). Coherent Expanded-Aerogels. *Journal of Physical Chemistry*, 36(1), 52–64. DOI: <https://doi.org/10.1021/j150331a003>

Klavariotia, M., Mantzavinos, D., & Kassinos, D. (2009). Removal of residual pharmaceuticals from aqueous systems by advanced oxidation processes. *Environment International*, 35, 402–417. DOI: <https://doi.org/10.1016/j.envint.2008.07.009>

Kodamatani, H., Tanisue, T., Fujioka, T., Kanzaki, R., & Tomiyasu, T. (2021). Inhibitory effect of alkyl groups on N-nitrosamine formation from secondary and tertiary alkylamines with monochloramine. *Environmental Technology & Innovation*, Volume 22, 101520. DOI: <https://doi.org/10.1016/j.eti.2021.101520>

Kraupner, N., Ebmeyer, S., Hutinel, M., Fick, J., Flach, C.-H., & Larsson, D. G. J. (2020). Selective concentrations for trimethoprim resistance in aquatic environments. *Environment International*, 144, 106083. DOI: <https://doi.org/10.1016/j.envint.2020.106083>

Kwarciak-Kozłowska, A. (2019). 7 - Removal of pharmaceuticals and personal care products by ozonation, advance oxidation processes, and membrane separation. *Pharmaceuticals and Personal Care Products: Waste Management and Treatment Technology (151-171)*, Oxford: Butterworth-Heinemann. DOI: <https://doi.org/10.1016/B978-0-12-816189-0.00007-X>

Lamy-Mendes, A., Pontinha, A. D. R., Alves, P., Santos, P., & Durães, L. (2021). Progress in silica aerogel-containing materials for buildings' thermal insulation.

*Construction and Building Materials*, 286, 122815. DOI: <https://doi.org/10.1016/j.conbuildmat.2021.122815>

Lee, C., Yoon, J., & von Gunten, U. (2007). Oxidative degradation of N-nitrosodimethylamine by conventional ozonation and the advanced oxidation process ozone/hydrogen peroxide. *Water Research*, 41, 581-590. DOI: <https://doi.org/10.1016/j.watres.2006.10.033>

Leventis, N., Chandrasekaran, N., Sotiriou-Leventisa, C., & Mumtaz, A. (2009). Smelting in the age of nano: iron aerogels. *Journals of Materials. Chemistry*, 19, 63-65. DOI: <https://doi.org/10.1039/B815985H>

Li, H., Zhou, Y., Tu, W., Ye, J., & Zou Z. (2015). State-of-the-art progress in diverse heterostructured photocatalysts toward promoting photocatalytic performance. *Adv Funct Mater*, 25, 998-1013. DOI: <https://doi.org/10.1002/adfm.201401636>

Liao, J., Liu, P., Xie, Y., & Zhang, Y. (2021). Metal oxide aerogels: preparation and application for the uranium removal from aqueous solution. *Science of The Total Environment*, 768, 144212. DOI: <https://doi.org/10.1016/j.scitotenv.2020.144212>

Liu, W., Rodriguez, P., Borchardt, L., Foelske, A., Yuan, J., Herrmann, A.-K., Geiger, D., Zheng, Z., Kaskel, S., Gaponik, N., Kötz, R., Schmidt, T. J., & Eychmüller, A. (2013). Bimetallic aerogels: high-performance electrocatalysts for the oxygen reduction reaction. *Angew. Chem. Int. Ed.*, 52, 9849-9852. DOI: <https://doi.org/10.1002/anie.201303109>

Lu, L., Sun, X., Ma, J., Yang, D., Wu, H., Zhang, B., Zhang, J., & Han, B. (2018). Highly Efficient Electroreduction of CO<sub>2</sub> to Methanol on Palladium-Copper Bimetallic Aerogels. *Angew. Chem. Int. Ed*, 57, 14149. DOI: <https://doi.org/10.1002/anie.201808964>

Luo, J., Zhang, S., Sun, M., Yang, L., Luo, S., & Crittenden, J. C. (2019). A critical review on energy conversion and environmental remediation of photocatalysts with remodeling crystal lattice, surface, and interface. *ACS Nano*, 13, 9811-9840. <https://doi.org/10.1021/acsnano.9b03649>

Luo, M., Wang, M., Pang, H., Zhang, R., Huang, J., Liang, K., Chen, P., Sun, P., & Kong, B. (2021). Super-assembled highly compressible and flexible cellulose aerogels for

methylene blue removal from water. *Chinese Chemical Letters*. DOI: <https://doi.org/10.1016/j.ccllet.2021.03.024>

Maida, J. (2021). *Top 5 Vendors in the Aerogel Market from 2016 to 2020: Technavio*. Retrieved from <https://bwnews.pr/3uk1x6n>

Maleki, H. (2016). Recent advances in aerogels for environmental remediation applications: a review. *Chemical Engineering Journal*, 300, 98-118. DOI: <https://doi.org/10.1016/j.cej.2016.04.098>

Manzocco, L., Mikkonen, K. S., & García-González, C. A. (2021). Aerogels as porous structures for food applications: smart ingredients and novel packaging materials. *Food Structure*, 28, 100188. DOI: <https://doi.org/10.1016/j.foostr.2021.100188>

Matoh, L., Žener, B., Korošec, R. C., & Štangar, U. L. (2019). 27 - Photocatalytic water treatment. In Pacheco-Torgal, F., Diamanti, M. V., Nazari, A., Granqvist, C. G., Pruna, A., & Amirkhanian, S. (Ed.). *Nanotechnology in Eco-efficient Construction (2<sup>nd</sup> ed. 675-702)*, Cambridge: Woodhead Publishing. DOI: <https://doi.org/10.1016/B978-0-08-102641-0.00027-X>

Mazrouei-Sebdani, Z., Begum, H., Schoenwald, S., Horoshenkov, K. V., & Malfait, W. J. (2021). A review on silica aerogel-based materials for acoustic applications. *Journal of Non-Crystalline Solids*, 562, 120770. DOI: <https://doi.org/10.1016/j.jnoncrysol.2021.120770>

Michalski, R. (2003). Toxicity of bromate ions in drinking water and its determination using ion chromatography with post column derivatisation. *Polish Journal of Environmental Studies*, 12(6), 727-734. Retrieved from <https://bit.ly/3yBN1tL>

Munter, R. (2001). Advanced oxidation processes – current status and prospects. *Proceedings of the Estonian Academy of Sciences*, 50, 59-80. Retrieved from <https://bit.ly/3yBkWCY>

Naskar, S., Freytag, A., Deutsch, J., Wendt, N., Behrens, P., Köckritz, A., & Bigall, N. C. (2017). Porous aerogels from shape-controlled metal nanoparticles directly from nonpolar colloidal solution. *Chemistry of Materials*, 29(21), 9208-9217. DOI: <https://doi.org/10.1021/acs.chemmater.7b03088>

National Center for Biotechnology Information (2021a). PubChem Compound Summary for CID 5921, N-Nitrosodiethylamine. Retrieved from <https://bit.ly/3uoFVpg>

National Center for Biotechnology Information (2021b). PubChem Compound Summary for CID 5578, Trimethoprim. Retrieved from <https://bit.ly/2TiCNyv>

Nazri, M. K. H. M., & Sapawe, N. (2020). A short review on photocatalytic reaction in diesel degradation. *Materials Today: Proceedings, Volume 31(1)*, A33-A37. DOI: <https://doi.org/10.1016/j.matpr.2020.10.965>

Oller, I., & Malato, S. (2021). Photo-Fenton applied to the removal of pharmaceutical and other pollutants of emerging concern. *Current Opinion in Green and Sustainable Chemistry, 29*, 100458. DOI: <https://doi.org/10.1016/j.cogsc.2021.100458>

Parsons, S. A., & Williams, M. (2004). Advanced oxidation processes for water and wastewater treatment. In Parsons S. (Ed.). (4), London, UK: IWA Publishing. DOI: <https://doi.org/10.2166/9781780403076>

Perez, J. J., Villanueva, M. E., Sánchez, L., Ollier, R., Alvarez, V., & Copello, G. J. (2020). Low cost and regenerable composites based on chitin/bentonite for the adsorption potential emerging pollutants. *Applied Clay Science, 194*, 105703. DOI: <https://doi.org/10.1016/j.clay.2020.105703>.

Pignatello, J. J., Oliveros, E., & Mackay, A. (2006). Advanced oxidation processes for organic contaminant destruction based on the Fenton reaction and related chemistry. *Critical Reviews in Environmental Science and Technology, 36(1)*, 1-84. DOI: <https://doi.org/10.1080/10643380500326564>

Plumlee, M. H., & Reinhard, M. (2007). Photochemical attenuation of N-nitrosodimethylamine (NDMA) and other nitrosamines in surface water. *Environmental Science & Technology, 41(17)*, 6170-6176. DOI: <https://doi.org/10.1021/es070818l>

Qin, Y., Hao, M., & Li, Z. (2020). Chapter 17 - Metal-organic frameworks for photocatalysis. In Yu, J., Jaroniec, M., & Jiang, C. (Ed.). (*Interface Science and Technology* (30, 541-579). Amsterdam: Elsevier. DOI: <https://doi.org/10.1016/b978-0-08-102890-2.00017-8>

Reny, R., Plumlee, M. H., Kodamatani, H., Suffet, I. H. M., & Roback, S. L. (2021). NDMA and NDMA precursor attenuation in environmental buffers prior to groundwater recharge for potable reuse. *Science of The Total Environment, Volume 762*, 144287. DOI: <https://doi.org/10.1016/j.scitotenv.2020.144287>

Rincón, G. J., & La Motta, E. J. (2019). A fluidized-bed reactor for the photocatalytic mineralization of phenol on TiO<sub>2</sub>-coated silica gel. *Heliyon*, 5(6), e01966. DOI: <https://doi.org/10.1016/j.heliyon.2019.e01966>

Roibu, A., Fransen, S., Leblebici, M. E., Meir, G., Van Gerven, T., & Kuhn, S. (2018) An accessible visible-light actinometer for the determination of photon flux and optical pathlength in flow photo microreactors. *Scientific Reports*, 8, 5421. Sci Rep 8, 5421 (2018). DOI: <https://doi.org/10.1038/s41598-018-23735-2>

Rosal, R., Rodríguez, A., Perdigón-Melón, J. A., Petre, A., & García-Calvo, E. (2009) Oxidation of dissolved organic matter in the effluent of a sewage treatment plant using ozone combined with hydrogen peroxide (O<sub>3</sub>/H<sub>2</sub>O<sub>2</sub>). *Chemical Engineering Journal*, 149, 311-318. DOI: <https://doi.org/10.1016/j.cej.2008.11.019>

Saleh, M., Bilici, Z., Kaya, M., Yalvac, M., Arslan, H., Yatmaz, H. C., & Dizge, N. (2021). The use of basalt powder as a natural heterogeneous catalyst in the Fenton and Photo-Fenton oxidation of cationic dyes. *Advanced Powder Technology*, 32, (4), 1264-1275. DOI: <https://doi.org/10.1016/j.appt.2021.02.025>

Sarawade, P. B., Kim, J.-K., Kim, H.-K., & Kim, H.-T. (2007). High specific surface area TEOS-based aerogels with large pore volume prepared at an ambient pressure. *Applied Surface Science*, 254 (2), 574-579. DOI: <https://doi.org/10.1016/j.apsusc.2007.06.063>

Sharpless, C. M., & Linden, K. G. (2003). Experimental and model comparisons of low- and medium-pressure Hg lamps for the direct and H<sub>2</sub>O<sub>2</sub> assisted UV photodegradation of N-nitrosodimethylamine in simulated drinking water. *Environmental Science and Technology*, 37(9) 1933-1940. DOI: <https://doi.org/10.1021/es025814p>

Shin, W.-T., Mirmiran, A., Yiacomini, S., & Tsouris, C. (1999). Ozonation using microbubbles formed by electric fields. *Separation and Purification Technology*, 15, 217-282. DOI: [https://doi.org/10.1016/S1383-5866\(98\)00107-5](https://doi.org/10.1016/S1383-5866(98)00107-5)

Stamm, C., Räsänen, K., Burdon, F. J., Altermatt, F., Jokela, J., Joss, A., Ackermann, M., & Eggen, R. I. L. (2016). Chapter four - Unravelling the impacts of micropollutants in aquatic ecosystems: interdisciplinary studies at the interface of large-scale ecology. In Dumbrell, A. J., Kordas, R. L., & Woodward G. (Ed.). *Advances in Ecological Research* (55, 183-223). DOI: <https://doi.org/10.1016/bs.aecr.2016.07.002>.

Tang, Y., Yeo, K. L., Chen, Y., Yap, L. W., Xiong, W., & Cheng, W. (2013). Ultralow-density copper nanowire aerogel monoliths with tunable mechanical and electrical properties. *Journal of Materials Chemistry A*, 1(23), 6723. DOI: <https://doi.org/10.1039/c3ta10969k>

University of York (2019). *Antibiotics found in some of the world's rivers exceed 'safe' levels, global study finds*. Retrieved from <https://bit.ly/3hUo8ns>

Vallribera, A., & Molins, E. (2007). Aerogel Supported Nanoparticles in Catalysis. In Astruc, D. (Ed.). *Nanoparticles and Catalysis*. DOI: <https://doi.org/10.1002/9783527621323.ch5>

Wang, R., Shan, G., Wang, T., Yin, D., & Chen, Y. (2021). Photothermal enhanced photocatalytic activity based on Ag-doped CuS nanocomposites. *Journal of Alloys and Compounds*, 864, 158591. DOI: <https://doi.org/10.1016/j.jallcom.2020.158591>

Wang, S., & Wang, J. (2017). *Trimethoprim degradation by Fenton and Fe(II)-activated persulfate processes*. *Chemosphere*, 191, 97-105. DOI: <https://doi.org/10.1016/j.chemosphere.2017.10.040>.

Wang, S. (2008). A Comparative study of Fenton and Fenton-like reaction kinetics in decolourisation of wastewater. *Dyes and Pigments*, 76(3), 714-720. DOI: <https://doi.org/10.1016/j.dyepig.2007.01.012>

Wen, D., Herrmann, A.-K., Borchardt, L., Simon, F., Liu, W., Kaskel, S., & Eychmüller, A. (2014). Controlling the growth of palladium aerogels with high-performance toward bioelectrocatalytic oxidation of glucose. *Journal of the American Chemical Society*, 136(7), 2727-2730. DOI: <https://doi.org/10.1021/ja412062e>

Wen, D., Liu, W., Haubold, D., Zhu, C., Oschatz, M., Holzschuh, M., Wolf, A., Simon, F., Kaskel, S., & Eychmüller, A. (2016). Gold aerogels: three-dimensional assembly of

nanoparticles and their use as electrocatalytic interfaces. *ACS Nano*, 10(2), 2559-2567. DOI: <https://doi.org/10.1021/acsnano.5b07505>

WHO (2019). *WHO model list of essential medicines - 21st list*. 2019WHO/MVP/EMP/IAU/2019.06 Retrieved from <https://bit.ly/2REN4EO>

WHO (2021). *Information Note Nitrosamine impurities*. Retrieved from <https://bit.ly/3wsPI4o>

Wilkinson, J., Hooda, P. S., Barker, J., Barton, S., & Swinden, J. (2017). Occurrence, fate and transformation of emerging contaminants in water: An overarching review of the field. *Environmental Pollution*, 231, 954–970. DOI: <https://doi.org/10.1016/j.envpol.2017.08.032>

Wu, R.-X., Yu, C.-M., Hsu, S.-T., & Wang, C. H. (2021). Emergence of concurrent levofloxacin- and trimethoprim/sulfamethoxazole-resistant *Stenotrophomonas maltophilia*: risk factors and antimicrobial sensitivity pattern analysis from a single medical center in Taiwan. *Journal of Microbiology, Immunology and Infection*. DOI: <https://doi.org/10.1016/j.jmii.2020.12.012>

Wu, Y., Huang, J., Chen, J., Li, D., Shi, X., Du, Y., & Deng, H. (2021). Ordered hollow nanofiber aerogel with revivability for efficient oil absorption. *Journal of Cleaner Production*, 290, 125789. DOI: <https://doi.org/10.1016/j.jclepro.2021.125789>

Xu, R., Liu, W., Cai, J., & Li, Z. (2021). Robust RGO composite aerogels with high adsorption capabilities for organic pollutants in water. *Separation and Purification Technology*, 257, 117876. DOI: <https://doi.org/10.1016/j.seppur.2020.117876>

Yao, C., Dong, X., Gao, G., Sha, F., & Dongyu, X. (2021). Microstructure and adsorption properties of MTMS / TEOS co-precursor silica aerogels dried at ambient pressure. *Journal of Non-Crystalline Solids*, 562, 120778. DOI: <https://doi.org/10.1016/j.jnoncrysol.2021.120778>

Yazdan-Abad, M. Z., Noroozifar, M., Douk, A. S., Modarresi-Alam, A. R., & Saravani, H. (2019). Shape engineering of palladium aerogels assembled by nanosheets to achieve a high performance electrocatalyst. *Applied Catalysis B: Environmental*, 250, 242-249. DOI: <https://doi.org/10.1016/j.apcatb.2019.02.064>

Zhou, H., & Smith, D. W. (2002). Advanced technologies in water and wastewater treatment. *Journal of Environmental Engineering and Science*, 1(4), 247–264. DOI: <https://doi.org/10.1139/s02-020>

Zhu, S., & Wang, D. (2017). Photocatalysis: Basic Principles, Diverse Forms of Implementations and Emerging Scientific Opportunities. *Advanced Energy Materials*, 7(23), 1700841. DOI: <https://doi.org/10.1002/aenm.201700841>

Zhu, Y., Fan, W., Feng, W., Wang, Y., Liu, S., Dong, Z., & Li, X. (2021). A critical review on metal complexes removal from water using methods based on Fenton-like reactions: analysis and comparison of methods and mechanisms. *Journal of Hazardous Materials*, 414, 125517. DOI: <https://doi.org/10.1016/j.jhazmat.2021.125517>